AGU PUBLICATIONS

Geophysical Research Letters

RESEARCH LETTER
10.1002/2015GL067439

Key Points:
- New 10 km grid of terrestrial gravity anomalies in Antarctica, covering 73% of the continent
- Enabling determination of new high-resolution combined Earth gravity models
- Providing new tool to investigate lithospheric structure and geological evolution of Antarctica

Supporting Information:
- Supporting Information S1

Correspondence to:
M. Scheinert,
mirko.scheinert@tu-dresden.de

Citation:
Scheinert, M., et al. (2016), New Antarctic gravity anomaly grid for enhanced geodetic and geophysical studies in Antarctica, *Geophys. Res. Lett.*, *43*, 600–610, doi:10.1002/2015GL067439.

Received 15 DEC 2015
Accepted 4 JAN 2016
Accepted article online 8 JAN 2016
Published online 21 JAN 2016

New Antarctic gravity anomaly grid for enhanced geodetic and geophysical studies in Antarctica

M. Scheinert[1], F. Ferraccioli[2], J. Schwabe[1,3], R. Bell[4], M. Studinger[5], D. Damaske[6], W. Jokat[7,8], N. Aleshkova[9], T. Jordan[2], G. Leitchenkov[9,10], D. D. Blankenship[11], T. M. Damiani[12], D. Young[11], J. R. Cochran[4], and T. D. Richter[11]

[1]Institut für Planetare Geodäsie, Technische Universität Dresden, Dresden, Germany, [2]British Antarctic Survey, Cambridge, UK, [3]Now at Bundesamt für Kartographie and Geodäsie, Leipzig, Germany, [4]Lamont-Doherty Earth Observatory, Columbia University, Palisades, New York, USA, [5]NASA Goddard Space Flight Center, Greenbelt, Maryland, USA, [6]Bundesanstalt für Geowissenschaften und Rohstoffe, Hannover, Germany, [7]Alfred-Wegener-Institut, Helmholtz-Zentrum für Polar-und Meeresforschung, Bremerhaven, Germany, [8]Geoscience Department, University of Bremen, Bremen, Germany, [9]VNIIOkeangeologia, Saint Petersburg, Russia, [10]Department of Geophysics, Saint Petersburg State University, Saint Petersburg, Russia, [11]Institute for Geophysics, Jackson School of Geosciences, University of Texas at Austin, Austin, Texas, USA, [12]National Geodetic Survey, NOAA, Silver Spring, Maryland, USA

Abstract Gravity surveying is challenging in Antarctica because of its hostile environment and inaccessibility. Nevertheless, many ground-based, airborne, and shipborne gravity campaigns have been completed by the geophysical and geodetic communities since the 1980s. We present the first modern Antarctic-wide gravity data compilation derived from 13 million data points covering an area of 10 million km^2, which corresponds to 73% coverage of the continent. The remove-compute-restore technique was applied for gridding, which facilitated leveling of the different gravity data sets with respect to an Earth gravity model derived from satellite data alone. The resulting free-air and Bouguer gravity anomaly grids of 10 km resolution are publicly available. These grids will enable new high-resolution combined Earth gravity models to be derived and represent a major step forward toward solving the geodetic polar data gap problem. They provide a new tool to investigate continental-scale lithospheric structure and geological evolution of Antarctica.

1. Introduction

The gravity field of the Earth is a key quantity of interest to geodesy and to other fields of geosciences. Being a distinguished equipotential surface of the gravity potential, the geoid serves as a reference surface for the realization of physical heights, which is an important task of geodesy [*Forsberg et al.*, 2005]. In oceanography the geoid serves as a reference for the determination of the (mean) sea surface topography. In polar regions where the ocean is partly covered by sea ice, icebergs, or ice shelves, the geoid also provides a link between the surface ellipsoidal height and the freeboard height, which in turn can be used to infer the thickness of the floating ice. Determining an equipotential surface is also of significance for Antarctic subglacial lake studies [*Ewert et al.*, 2012]. In geophysics, analyses of gravity anomalies yield insight into the structure of the lithosphere and into tectonic and geodynamic processes that shape the continents and surrounding oceans.

Huge progress in mapping the global Earth gravity field has been made in recent years aided in particular by the satellite gravity missions GRACE (Gravity Recovery and Climate Experiment) and GOCE (Gravity field and steady state Ocean Circulation Explorer) which enable a coherent coverage and consistent accuracy up to an unprecedented resolution of 130 km and 90 km, respectively. This long- to medium-wavelength field resolved by satellite gravimetry is of considerable usefulness to study deeper lithospheric features or large-scale regional- to continental-scale geoid patterns. However, it is the terrestrial data that critically augment our knowledge of the shorter-wavelength anomalies which are a key for studying crustal features and for a higher-resolution view of the geoid. In order to obtain such a higher resolution (up to 10 km) terrestrial gravity compilations can be utilized over most continents and oceans, including the Arctic [*Kenyon et al.*, 2008]. However, Antarctica remains the most difficult-to-access region on Earth and, therefore, still suffers from considerable gravity data coverage gaps. Nevertheless, over the years a considerable number of

gravity surveys have successfully been completed in Antarctica. Aerogravimetry, in particular, has enabled a huge step forward in Antarctic data coverage.

While major efforts have been made to compile all available Antarctic bedrock topography [*Fretwell et al.*, 2013] and magnetic data [*Golynsky et al.*, 2013], no modern continental-scale compilation of gravity data exists to date. Recognizing the pressing need for such a gravity compilation, in 2003 the International Association of Geodesy (IAG) launched an initiative which is now organized within Subcommission 2.4f "Gravity and Geoid in Antarctica" (AntGG). Here we present the major outcome of this international multidisciplinary initiative, the first continental-scale gravity anomaly grid for Antarctica.

Enhanced geodetic applications include the development of next generation Earth gravity models and a new Antarctic geoid derivation, while geophysical studies will greatly benefit from these gravity grids, too. A higher-resolution crustal thickness and elastic thickness estimation will become possible by combining gravity and seismic data compilations [*Ferraccioli et al.*, 2011; *An et al.*, 2015]. The gravity compilation will also shed new light onto the extent of major sedimentary basins and provides a new foundation to study the architecture and the evolution of the continent, including the processes of subduction, collision, continental rifting, and intraplate features.

2. Gravity Surveys in Antarctica

The acquisition of terrestrial gravity data in Antarctica is challenging because the continent and its surrounding ocean represent a hostile and remote environment. Conventional marine and land gravity surveying techniques are limited by sea ice and ice shelves and by the vast extension, remoteness, and inaccessibility of the Antarctic ice sheet, respectively. Most surveying activities are restricted to the Antarctic summer season, but adverse weather conditions can occur also during the summer, making ground operations challenging. Moreover, major logistic efforts are required to realize Antarctic surveys. Airborne gravimetry is the only viable method which is capable of dealing with these conditions and enables much larger areas to be surveyed in one season. Airborne surveys often comprise a suite of geophysical-geodetic equipment such as gravimeters, magnetometers to measure the Earth's near-lithosphere magnetic field, radio echo sounding (RES) to measure internal ice layers and subglacial topography, lasers to measure ice surface height and roughness, inertial navigation system (INS) to measure aircraft attitude and support the determination of the flight trajectory, and global navigation satellite system (GNSS) antennas and receivers to derive the flight trajectory and kinematic accelerations.

The International Polar Year 2007/2008 [*Krupnik et al.*, 2011] provided a springboard to launch major new airborne geophysical surveys, including airborne gravimetry over largely unexplored Antarctic frontiers, such as the Gamburtsev Subglacial Mountains [*Ferraccioli et al.*, 2011; *Bell et al.*, 2011] and Wilkes Land in East Antarctica [*Aitken et al.*, 2014]. Another project providing extensive new airborne gravity data coverage for Antarctica is NASA's Operation IceBridge that aims to bridge the gap between the satellite laser altimetry missions ICESat and ICESat-2 [*Studinger et al.*, 2010]. In East Antarctica a long-term airborne project was conducted by German institutions to unravel the largely unexplored Dronning Maud Land [*Riedel et al.*, 2012]. Over time a large number of gravimetric data sets have been collected in Antarctica by the international geosciences community and incorporated into the AntGG database that is being maintained at TU Dresden [*Scheinert*, 2012].

These gravity data differ in a number of aspects. Gravimetric surveys were initiated by different nations, and programs had different scientific goals and were realized at different observation epochs (see Table S1 in the supporting information). Depending on the applied technique and the positioning method, the accuracy of the gravity data differs over a large range. Issues like the realization of the gravimetric datum or survey layout to enable cross-over calibration also have a strong impact on the final accuracy of an individual survey. The raw data have been treated in different ways, especially with respect to filtering, reductions and/or corrections. For airborne surveys several issues can arise such as an unclear altitude reference of the data or whether a downward continuation was applied or not. These issues are also reflected in incomplete metadata for some of these surveys. In some cases it is also not clear if the term gravity anomaly is correctly referred to, or if—in the geodetic understanding—the data are given as gravity disturbances [*Hackney and Featherstone*, 2003]. Overlapping or complementary data sets may be internally consistent but can still contain systematic biases such as offsets and tilts. Thus, the large heterogeneity of the gravity data was carefully considered in our new Antarctic compilation.

Overall, more than 13 million gravity data points have been compiled in the AntGG database, originating from terrestrial, airborne, and shipborne surveys. More than one million line kilometers of aerogravimetry data are included in our new compilation effort. Altogether, the data compilation covers an area of 10 million km^2, corresponding to about 73% of the Antarctic continent including ice shelves. The oceanic area covered by gravity data corresponds to approximately 29% of the Southern Ocean south of 60°S.

3. Global High-Resolution Determination of the Gravity Field of the Earth

Global Earth Gravity Models (EGM) are based on satellite data. To obtain a higher resolution than such *satellite-only* models, terrestrial gravity data have to be included globally which leads to so-called *combined* EGMs. The term terrestrial data is used here to denote data of ground-based, airborne, and shipborne surveys. Combined EGMs reach a half-wavelength resolution of 70 km and better, comparable to harmonic degree and order (d/o) 360 and higher (for the relation of degree and resolution, see *Barthelmes* [2013, p. 20]). Recent high-resolution combined EGMs such as EGM2008 [*Pavlis et al.*, 2008] or EIGEN-6C4 [*Förste et al.*, 2014] reach a resolution of approximately 10 km (d/o 2190) over most parts of the world. However, in Antarctica the resolution is much lower due to two facts: First, the deviation of the satellite orbit inclination from 90° leads to a polar gap in satellite data. Second, the largest terrestrial data gaps still exist in Antarctica.

New satellite-based data provide unprecedented accuracy and resolution in the representation of the Earth's gravity field. The geodetic satellite mission GRACE (Gravity Recovery and Climate Experiment) has been in orbit since March 2002 [*Tapley et al.*, 2004] while GOCE (Gravity field and steady state Ocean Circulation Explorer) was launched in March 2009 and fell from orbit in November 2013 [*Floberghagen et al.*, 2011; *van der Meijde et al.*, 2015]. GRACE-based satellite-only global EGMs reach a resolution of 160 to 130 km (d/o 160 to 200), e.g., GGM05S [*Tapley et al.*, 2014]. GOCE has provided significantly higher-resolution data to satellite-only EGM. For example, EIGEN-6S2 [*Rudenko et al.*, 2014] combines LAGEOS laser-ranging data for the lower degrees 2–30, GRACE range rate data up to d/o 180, and GOCE data resulting in approximately 90 km resolution (d/o 260). However, GOCE has a polar data gap larger than that of GRACE with a diameter of approximately 1400 km due to its inclination of 96.5°. Therefore, to obtain a stabilized EGM solution, one has to apply a certain type of regularization [*Metzler and Pail*, 2005; *Pail et al.*, 2011] or to include terrestrial gravity data. However, the latter is not possible yet for Antarctica due to the lack of a continental-scale compilation.

4. Regional Gravity Field Determination in Antarctica and Choice of Background EGM

In regional gravity field determination the remove-compute-restore (RCR) technique is commonly applied [*Forsberg*, 1993; *Forsberg and Tscherning*, 1997; *Sansò and Sideris*, 2013]. However, as discussed in section 2, Antarctic gravity data exhibit large heterogeneities and inconsistencies. How heterogeneous gravity data can be utilized to improve the regional geoid has previously been presented for the Weddell Sea [*Schwabe and Scheinert*, 2014] and Lake Vostok [*Schwabe et al.*, 2014]. The application of a background EGM is a major step of the RCR technique (see section 5.2).

For this, a satellite-only EGM has to be used since it is independent from terrestrial data. GOCE-based EGMs are favorable for they enable the highest resolution. However, one has to deal with the polar data gap problem. Therefore, the reliability and the applicability of any GOCE-based EGM in the Antarctic interior depends considerably on the regularization technique used in the spherical harmonic analysis. Different approaches are applied in the determination of EGMs such as the European Space Agency's (ESA) direct, timewise, and spacewise models [*Pail et al.*, 2011] or the family of EIGEN [*Rudenko et al.*, 2014; *Shako et al.*, 2014] and GOCO [*Pail et al.*, 2010; *Mayer-Gürr*, 2012] models. GRACE data were merged up to a certain degree and order to deal with the poor sensitivity of GOCE gravity gradient measurements at long wavelengths. A spherical cap regularization [*Metzler and Pail*, 2005] was computed in an iterative way as in the ESA direct model ESA-DIR/R5 [*Bruinsma et al.*, 2013, 2014]. (For the sake of briefness, short abbrevations shall be used, like ESA-DIR/R5 for GO_CONS_GCF_2_DIR_R5, ESA's direct model release 5, and so on.) For the ESA-TIM/R5 a regularization was applied using synthetic signal degree variances due to Kaula's rule of thumb to constrain zonal and near-zonal coefficients that suffer mostly from the polar data gap [*Brockmann et al.*, 2014].

To investigate the performance of recent EGMs, a comparison was carried out using high-resolution airborne gravity data that can be regarded as providing ground truth for these global models. Our evaluation

(see Text S2 in the supporting information) considered regions both inside and outside the polar data gap. We concluded that the GOCO03S model [*Mayer-Gürr*, 2012] utilizes the GOCE observations in an appropriate way with minimum degradation of signals including the interior of the polar gap (which is due to the inclusion of GRACE data). Therefore, it is an appropriate choice to apply GOCO03S as a background EGM to serve as the common reference in adjusting the terrestrial Antarctic gravity data sets.

5. Derivation of a New Antarctic Gravity Anomaly Grid

In the compilation we focus primarily on continental surveys in order to close data gaps as best as currently possible. The original gravity data sets made available to AntGG comprise pointwise data, profile-wise data (as it is mostly the case for airborne and shipborne surveys), and gridded data sets. The original preprocessed gravity data were preserved as much as possible. In view of the large amount of data records (see section 2), and due to the generally poor linkage between the different data sets we did not attempt to mitigate all problematic issues in the individual data sets.

Shipborne data are only considered in some regions, since in general they show big gaps, incomplete metadata, and sometimes unclear referencing. Also, they are not that crucial since in the ocean areas satellite altimetry allows to derive adequate gravity information for most geodetic and geophysical applications [*Andersen et al.*, 2014; *Sandwell et al.*, 2014].

5.1. Compilation of Gravity Data and Metadata

For every campaign metadata were compiled as accurately as possible. The reliability of this process depends to a large extent on the information provided with the original gravity data sets. As a general rule, data of airborne surveys (where a GNSS referenced trajectory is available) were assigned gravity disturbances δg (cf. section 2), while shipborne and land data were treated as gravity anomalies Δg. In most of the surveys the gravity formula of GRS80 [*Moritz*, 1984] was taken to compute normal gravity. Where the older GRS67 formula was used, we applied a correction term [*Anderson et al.*, 1984] which almost results in a constant offset on the level of 1mGal. If the gravity reference is unknown (because it was not possible to connect to an absolute gravity point), a bias was introduced. As reference surface for ellipsoidal heights, the WGS84 ellipsoid [*NIMA*, 2000] was taken (which is the standard for GNSS positioning; deviations from the GRS80 ellipsoid can be neglected).

To characterize the accuracy of each individual data set—and to make the data sets comparable to each other at least in a relative sense—an a priori standard deviation σ_0 was allocated to each data set. In some cases it could be deduced from the metadata. If no information was available, we utilized precomparisons like cross-over computations or previous investigations incorporating independent data, see, e.g., *Schwabe and Scheinert* [2014]. Thus, a standard value of 3mGal was allocated to airborne gravity surveys where no other value was given. The spatial resolution of airborne campaigns depends mainly on the line spacing which varies from typically only a few kilometers to 30 km (see Table S1). Aircraft speed and respective filtering limit the along-line resolution which, however, is normally still higher than that resulting from the line spacing. Whereas the ground-based surveys ADGRAV-ROSS #23 and GEOMAUD #24 are assigned a priori standard deviations of 5mGal and 1mGal, respectively, the BAS survey #25 was given a higher value of 20mGal according to previous investigations [*Schwabe et al.*, 2012]. The PMGE/VNIIO compilation #26 was assigned a value of 10mGal since the data were mostly acquired before GNSS positioning became available. Also, due to unknown smoothing and gridding procedure this data set exhibits a lower spatial resolution of about 25 to 30km and biases of up to 25mGal (see also *Studinger* [1998] and *Schwabe and Scheinert* [2014]).

Information on the data sets incorporated into the Antarctic gravity anomaly grid are summarized in Table S1, including metadata and a priori standard deviation σ_0. In case of aerogravimetry, approximate total length of survey flights per campaign and line spacing are given. The individual gravimetric surveys are not discussed in this paper. Instead, one may refer to the relevant references reported in Table S1. Figure S1 shows location and spatial extension of the individual data sets. Multiple coverage of same areas by different surveys leads to overlaps as illustrated in Figure S2.

5.2. Processing and Gridding Procedure

From the mostly irregularly distributed data a regular gravity anomaly grid needed to be derived. To facilitate gridding on an equidistant rectangular grid centered at the South Pole we used the polar stereographic projection (based on the WGS84 ellipsoid, true scale at parallel 71°S, using Generic Mapping Tools (GMT) [*Wessel et al.*, 2013]). The grid spacing was chosen to be 10km. Due to uncertainties and heterogeneities in the data as

well as due to signal damping with increasing flight height and heterogeneous line spacing of aerogravimetry, a higher-resolution grid mesh was not warranted at continental scale. The choice of a 10 km grid mesh provides a reasonable compromise between the older, more widely spaced, ground-based surveys and newer and higher-resolution airborne geophysical campaigns.

Biases of the individual data sets were taken into account as well as the heterogeneous accuracy by introducing an a priori standard deviation for each data set. To consider these aspects accordingly the RCR technique is utilized which is a common method of physical geodesy (section 4). The RCR technique uses a *residual* disturbing potential δT which enables to apply spherical approximations and linearized functionals. The residual disturbing potential is made up of the remainder after the long-wavelength part is accounted for by a global EGM, and the short-wavelength part is accounted for by topography. Here we are using solely (irregularly distributed) gravity anomalies which can be regarded as a functional F of T, i.e., $\Delta g = F(T)$. Thus, the remove step reads

$$F(\delta T) = F(T) - F(T_{\mathrm{EGM}}) - F(T_{\mathrm{topo}}) \tag{1}$$

Subsequently, a compute step is applied to the residual functional which should be formally denoted by $\mathbf{C}$

$$[F(\delta T)] = \mathbf{C}\, F(\delta T) \tag{2}$$

Normally, on the left-hand side of this equation δT is standing alone. For example, in case of solving the gravimetric boundary value problem, $\mathbf{C}$ might designate the (modified) Stokes integral. Now, the parentheses [*] shall denote values given at the regular grid. After the compute step, the long-wavelength part and short-wavelength part are restored in the grid points:

$$[F(T)] = [F(\delta T)] + [F(T_{\mathrm{EGM}})] + [F(T_{\mathrm{topo}})] \tag{3}$$

As background EGM in the remove and restore steps (equations (1) and (3), respectively) GOCO03S [*Mayer-Gürr*, 2012] was used up to d/o 250. Topography is usually considered in a residual terrain model (RTM) approach which should have a smoothing effect on the data [*Forsberg and Tscherning*, 1997]. Here we carried out test calculations using the latest publicly available Bedmap2 compilation [*Fretwell et al.*, 2013] including both ice surface heights and bedrock topography. However, the resulting residual anomalies did not represent an improvement over residual free-air anomalies. Where Bedmap2 has lower accuracies (data void areas or areas with accuracies of only some hundred or even thousand meters), errors in bedrock topography would directly enter into residual gravity. Therefore, we decided not to apply the topographic reduction (in the RTM sense). Thus, the entire procedure comprises the following steps:

1. *Remove step.* The contribution of the background EGM (GOCO03S) was computed in each observation point at flight altitude (if given, see Table S1) or at the surface and subsequently subtracted from the original data (equation (1)). As a result of this step, we obtain residual gravity anomalies $\delta(\Delta g)^{(i)}$ for each individual survey (i) still given at irregularly distributed observation points. Gravity disturbances (where clearly identified) were converted to gravity anomalies in advance, estimating the difference $(\Delta g - \delta g)$ using the same EGM. At the long wavelengths the downward continuation is implicitly done using the EGM. A further step of downward continuation was not considered. Most data were taken at the surface or close to the surface anyway, as also airborne surveys were flown in altitudes such that the height above ground was small. It can be shown that the vertical gradient of residual gravity anomalies at flight altitude is close to zero and that the remaining effect of the downward continuation is of the order of magnitude of less than 0.1 mGal with a standard deviation of less than 1 mGal. Moreover, it should be emphasized that most airborne surveys were conducted over the Antarctic ice sheet, which means that ice thickness still adds to the distance from the ground (the ice surface) to bedrock topography. (The Antarctic ice sheet has a mean thickness of 2126 m [*Fretwell et al.*, 2013].)
2. *Compute step—Project.* This step is also done for each data set individually. The observation points originally given by geographical coordinates were mapped by polar stereographic projection into points on the plane. Then, the residual gravity anomalies were interpolated from the irregularly distributed points onto a regular grid with 10 km spacing. For this, we used the Generic Mapping Tool (GMT) [*Wessel et al.*, 2013].

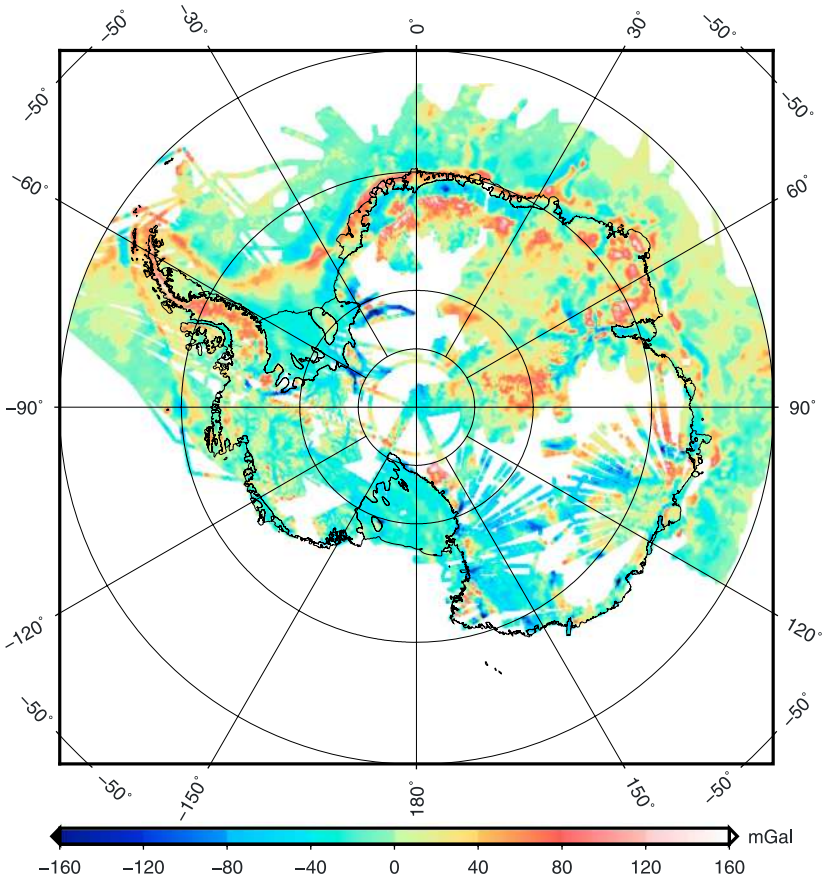

Figure 1. Gridded data set of surface free-air gravity anomalies in Antarctica.

Routine `blockmean` was used as a preprocessing step to avoid aliasing of shorter wavelengths. It computes the mean position and mean value for every grid cell that is not empty. After that, routine `surface` was applied to realize the interpolation to the regular grid. This is accomplished by solving

$$(1 - t) \cdot \Delta_s(\Delta_s z) + t \cdot \Delta_s z = 0 \tag{4}$$

where Δ_s denotes the surface Laplacian operator, t a tension factor [*Wessel and Smith*, 2015], and $z = z(x, y)$ the data to be gridded at rectangular coordinates, i.e., residual gravity anomalies given in terms of polar stereographic coordinates. A nonzero tension factor relaxes the constraint of minimum curvature that otherwise can result in "undesired oscillations" and "false local maxima and minima" [*Smith and Wessel*, 1990]. It is recommended to use values of $0.25, \ldots, 0.3$ for potential field data, whereas a larger tension factor (0.35) should be used for topography data [*Wessel and Smith*, 2015]. Here a tension factor of 0.3 was utilized. Depending on the respective (mean) spacing, a mask was derived for each data set considering its effective coverage in order to prevent gaps between profiles or single observation points. Gridded residual gravity anomalies $[\delta(\Delta g)^{(i)}]$ are resulting from this step. Their statistics are given in Table S2.

3. *Compute step—Level.* In subtracting the respective mean from the residual gravity anomalies (cf. Table S2) each data set (i) is individually referenced to the background EGM. In this way, systematic effects are accounted for, e.g., biases originating from different gravity datum realizations. This simple ansatz gives comparable results to a more complex computation using least squares estimation including the estimation of offsets as realized by *Schwabe and Scheinert* [2014]. Considerable offsets of up to 40mGal were detected. A higher-order detrending was also tested but omitted, since it can cause additional tilts or a degradation of the relative consistency between two overlapping data sets. As a result, leveled residual gravity anomalies $[\delta(\Delta g)_0^{(i)}]$ are obtained.

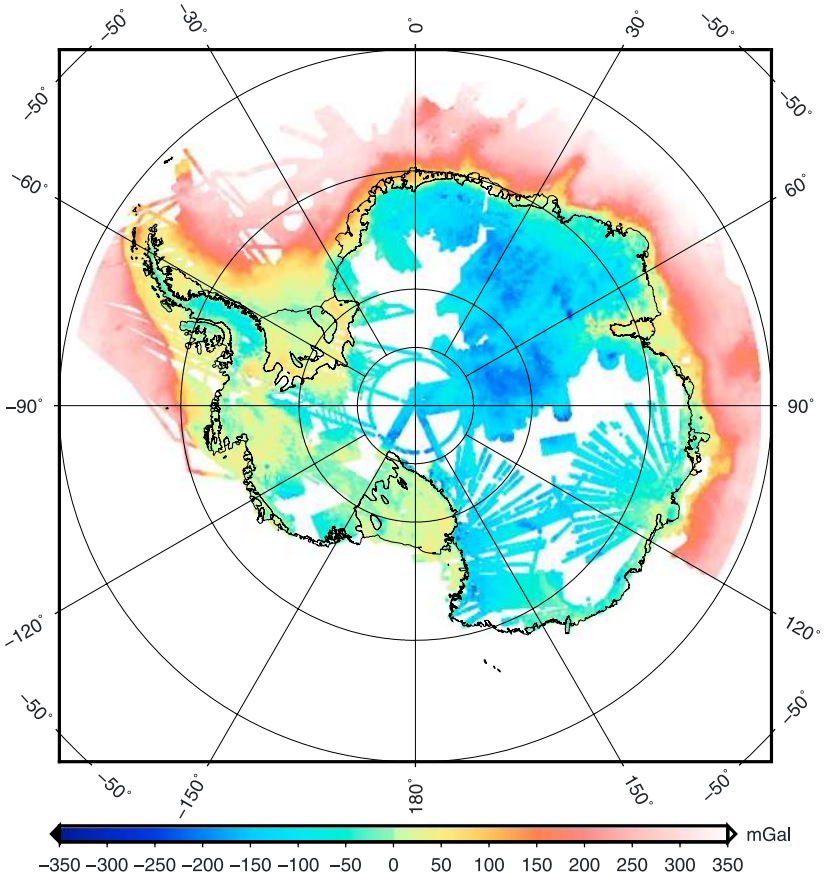

Figure 2. Gridded data set of complete Bouguer gravity anomalies in Antarctica using Bedmap2 [*Fretwell et al.*, 2013]. See section 5.3 for explanations.

4. *Compute step — Merge.* Up to this step the data sets were treated individually. According to coverage, leveled residual gravity anomalies $[\delta(\Delta g)_0^{(i)}]$ of more than one survey could be given in one grid point. Now the final value is computed by a pointwise weighted mean from the individual gridded residual gravity anomalies:

$$[\delta(\Delta g)] = \frac{\sum p_i [\delta(\Delta g)_0^{(i)}]}{\sum p_i} \tag{5}$$

Weights were derived taken inverse a priori variances (Table S1): $p_i = 1/\sigma_i^2$. Edge effects may occur where multiple data sets of different accuracy intersect or overlap. However, a filtering was not applied in order not to propagate such effects more widely throughout the grid. This step results in a regular grid of residual gravity anomalies $[\delta(\Delta g)]$.

5. *Restore step.* The contribution of the background EGM is restored according to equation (3). This was accomplished by adding the long-wavelength part evaluated from the background EGM in the points of the regular grid at the surface. This results in the desired regular grid of gravity anomalies $[\Delta g]$.

5.3. Results

The resulting gridded data set of (surface) gravity anomalies is the main outcome. In Figure 1 the planar grid was mapped to geographic coordinates by means of inverse polar stereographic projection. Figure S1 gives the root-mean-square (RMS) of the weighted mean, propagated from a priori standard deviations as listed in Table S1.

To evaluate the impact of newer aerogravimetry data, the RMS of residual individual data sets was estimated with respect to the residual gridded data set (Figure S3). For example, this map clearly demonstrates the consistency of IceBridge data (#22) with other overlapping aerogravimetric data, e.g., in the Weddell Sea and Antarctic Peninsula regions and also at higher latitudes closer to the pole. Vice versa, larger deviations can be detected for the PMGE/VNIIO compilation #26 in East Antarctica (between 60°E and 90°E). A major reason

for the lower accuracy lies in the fact that a lot of the data incorporated into this compilation were acquired prior to the availability of GNSS positioning. In the region of the Antarctic Peninsula, larger deviations are partly due to data set #25 (see discussion in section 5.1). Here an improvement is likely to occur when accurate topography information is incorporated into the RCR processing scheme.

Finally, from the gridded gravity anomalies, complete Bouguer anomalies (Figure 2) were computed making use of the Bedmap2 data set [*Fretwell et al.*, 2013]. For this, the GRAVSOFT routine TC [*Forsberg and Tscherning*, 2008] was utilized applying a spherical prism integration with an integration radius of 300 km. To compute the complete Bouguer anomaly all density discontinuities were taken into account, with (standard) densities of 2670 kg/m^3 for rock, 917 kg/m^3 for ice, and 1025 kg/m^3 for water.

6. Implications for Antarctic Geophysics

Our compilation of gravity anomalies provides a new basis for the geophysical community to study large-scale crustal architecture, effective elastic thickness, and isostatic and tectonic processes that shaped the Antarctic continent from the Precambrian to the Cenozoic. The continental-scale gravity compilation will also assist in developing more robust geophysical ties between Antarctica and formerly adjacent continents within the Gondwana, Rodinia, and Columbia supercontinents [*Aitken et al.*, 2016].

Recent continental-scale estimations of crustal thickness variations beneath Antarctica have relied mainly on inversions of satellite gravity [*Block et al.*, 2009; *O'Donnell and Nyblade*, 2014] or compilations of relatively sparse and mostly passive seismic arrays [*An et al.*, 2015]. Our new free-air and Bouguer anomaly grids are capable of resolving much shorter wavelength features related, for example, to major sedimentary basins and other intracrustal density variations. By incorporating the more regional-scale flexural responses to these intracrustal loads [*Watts*, 2001], improved crustal thickness estimations and tectonic interpretations for Antarctica will in turn become possible. Deriving improved estimates of crustal and sedimentary basin thickness in Antarctica is important in the quest to better constrain geothermal heat flux variations [*Maule et al.*, 2005] and quantify their potential influence on subglacial hydrology and ice sheet dynamics [*Bell et al.*, 1998; *Schroeder et al.*, 2014]. Efforts to select the ideal candidate sites for drilling the oldest ice [*Fischer et al.*, 2013] also require an improved knowledge of the crustal structure in East Antarctica, which can influence regional geothermal heat flux patterns and hence the preservation of old basal ice.

The first terrestrial gravity anomaly grids for Antarctica will help shed new light onto the evolution of fundamental large-scale geological processes such as continental rifting in West Antarctica [*Damiani et al.*, 2014; *Jordan et al.*, 2013a; *Bingham et al.*, 2012; *Jordan et al.*, 2010] and intraplate mountain building in the Transantarctic Mountains [*Stern and ten Brink*, 1989; *Studinger et al.*, 2004, 2006; *Jordan et al.*, 2013b], the Gamburtsev Subglacial Mountains [*Ferraccioli et al.*, 2011], and Dronning Maud Land [*Näslund*, 2001]. Gravity anomalies can aid studies of subduction and terrane accretion processes [*Ferraccioli et al.*, 2002, 2006] and intraplate basin formation [*Ferraccioli et al.*, 2009]. The availability of new terrestrial gravity anomaly grids for Antarctica will also augment current international efforts to compile almost two million line kilometers of recent magnetic anomaly data for the continent [*Golynsky et al.*, 2013] and together with these data, will provide a window on Antarctic subglacial geology and tectonic evolution [*Jokat et al.*, 2003; *Riedel and Jokat*, 2007; *Ferraccioli et al.*, 2009; *Aitken et al.*, 2014].

7. Conclusions and Outlook

The first Antarctic-wide gridded data set of gravity anomalies has been derived by incorporating all available gravity data collected over the continent over the last three decades. In the gridding procedure our aim was to preserve, as much as possible, the features of the original data sets (namely, accuracy and variability). The scientific user is provided the grids of (surface) free-air gravity anomalies and of Bouguer anomalies with a grid spacing of 10 km each as well as a grid of accuracy measures (propagated RMS). The Antarctic gravity anomaly grid is ready to be used in the derivation of new global Earth Gravity Models. Also, as a next step of AntGG, an improved continent-wide Antarctic regional geoid will be derived from our new grid. Although the data coverage is still partially incomplete, the new compilation represents the biggest step forward so far toward solving the polar data gap problem. Further gravity surveys (especially airborne campaigns) are to be carried out, especially over the South Pole region, the largest of the gaps that is of significant hindrance, in particular, for global models derived from GOCE data. As several international projects are planned in this respect, there

is a high probability that the remaining major data gaps will be closed within the next few years. In the course of time, with new data being available, it is anticipated to provide updates of the Antarctic gravity anomaly grid presented here.

Data sets are available at https://doi.org/10.1594/PANGAEA.848168.

Acknowledgments
All contributors of gravity data are greatly acknowledged. M.S. thanks all colleagues who have supported the work of AntGG during the last decade, either as active members in the IAG Subcommission 2.4f "Gravity and Geoid in Antarctica" and/or in the SCAR Expert Group GIANT or in other ways of collaboration. We thank two anonymous reviewers for their valuable remarks that helped to improve the manuscript.

References

Aitken, A., P. Betts, D. Young, D. Blankenship, J. Roberts, and M. Siegert (2016), The Australo-Antarctic Columbia to Gondwana transition, *Gondwana Res.*, *29*(1), 136–152, doi:10.1016/j.gr.2014.10.019.

Aitken, A. R. A., D. A. Young, F. Ferraccioli, P. G. Betts, J. S. Greenbaum, T. G. Richter, J. L. Roberts, D. D. Blankenship, and M. J. Siegert (2014), The subglacial geology of Wilkes Land, East Antarctica, *Geophys. Res. Lett.*, *41*, 2390–2400, doi:10.1002/2014GL059405.

An, M., D. A. Wiens, Y. Zhao, M. Feng, A. A. Nyblade, M. Kanao, Y. Li, A. Maggi, and J.-J. Lévêque (2015), S-velocity model and inferred Moho topography beneath the Antarctic Plate from Rayleigh waves, *J. Geophys. Res. Solid Earth*, *120*, 359–383, doi:10.1002/2014JB011332.

Andersen, O. B., P. Knudsen, S. Kenyon, and S. Holmes (2014), Global and Arctic marine gravity field from recent satellite altimetry (DTU13),paper presented at 76th EAGE Conference and Exhibition, doi:10.3997/2214-4609.20140897.

Anderson, D. L., et al. (1984), Geophysik der festen Erde, des Mondes und der Planeten, *Landolt-Börnstein, Neue Serie, Gruppe V: Geophysik und Weltraumforschung*, vol. 2a, edited by K. Fuchs and H. Soffel, p. 335, Springer, Berlin, Heidelberg, New York.

Barthelmes, F. (2013), Definition of functionals of the geopotential and their calculation from spherical harmonic models, Sci. Techn. Rep. STR09/02, Helmholtz-Zentrum Potsdam Deutsches GeoForschungsZentrum, Potsdam, (revised ed.), Po.

Bell, R. E., D. D. Blankenship, C. A. Finn, D. L. Morse, T. A. Scambos, J. M. Brozena, and S. M. Hodge (1998), Influence of subglacial geology on the onset of a West Antarctic ice stream from aerogeophysical observations, *Nature*, *394*, 58–62, doi:10.1038/27883.

Bell, R. E., et al. (2011), Widespread persistent thickening of the East Antarctic ice sheet by freezing from the base, *Science*, *331*(6024), 1592–1595, doi:10.1126/science.1200109.

Bingham, R. G., F. Ferraccioli, E. C. King, R. D. Larter, H. D. Pritchard, A. M. Smith, and D. G. Vaughan (2012), Inland thinning of West Antarctic ice sheet steered along subglacial rifts, *Nature*, *487*(7408), 468–471, doi:10.1038/nature11292.

Block, A. E., R. E. Bell, and M. Studinger (2009), Antarctic crustal thickness from satellite gravity: Implications for the Transantarctic and Gamburtsev Subglacial Mountains, *Earth Planet. Sci. Lett.*, *288*(1–2), 194–203, doi:10.1016/j.epsl.2009.09.022.

Brockmann, J. M., N. Zehentner, E. Höck, R. Pail, I. Loth, T. Mayer-Gürr, and W.-D. Schuh (2014), EGM_TIM_RL05: An independent geoid with centimeter accuracy purely based on the GOCE mission, *Geophys. Res. Lett.*, *41*, 8089–8099, doi:10.1002/2014GL061904.

Bruinsma, S. L., C. Förste, O. Abrikosov, J.-C. Marty, M.-H. Rio, S. Mulet, and S. Bonvalot (2013), The new ESA satellite-only gravity field model via the direct approach, *Geophys. Res. Lett.*, *40*, 3607–3612, doi:10.1002/grl.50716.

Bruinsma, S. L., C. Foerste, O. Abrikosov, J.-M. Lemoine, J.-C. Marty, S. Mulet, M.-H. Rio, and S. Bonvalot (2014), ESA's satellite-only gravity field model via the direct approach based on all GOCE data, *Geophys. Res. Lett.*, *41*, 7508–7514, doi:10.1002/2014GL062045.

Damiani, T. M., T. A. Jordan, F. Ferraccioli, D. A. Young, and D. D. Blankenship (2014), Variable crustal thickness beneath Thwaites Glacier revealed from airborne gravimetry, possible implications for geothermal heat flux in West Antarctica, *Earth Planet. Sci. Lett.*, *407*, 109–122, doi:10.1016/j.epsl.2014.09.023.

Ewert, H., S. Popov, A. Richter, J. Schwabe, R. Dietrich, and M. Scheinert (2012), Precise analysis of ICESat altimetry data and assessment of the hydrostatic equilibrium for subglacial Lake Vostok, East Antarctica, *Geophys. J. Int.*, *191*, 557–568, doi:10.1111/j.1365-246X.2012.05649.x.

Ferraccioli, F., E. Bozzo, and G. Capponi (2002), Aeromagnetic and gravity anomaly constraints for an early Paleozoic subduction system of Victoria Land, Antarctica, *Geophys. Res. Lett.*, *29*(10), 1406, doi:10.1029/2001GL014138.

Ferraccioli, F., P. Jones, A. Vaughan, and P. Leat (2006), New aerogeophysical view of the Antarctic Peninsula: More pieces, less puzzle, *Geophys. Res. Lett.*, *33*, L05310, doi:10.1029/2005GL024636.

Ferraccioli, F., E. Armadillo, T. Jordan, E. Bozzo, and H. Corr (2009), Aeromagnetic exploration over the East Antarctic ice sheet: A new view of the Wilkes Subglacial Basin, *Tectonophysics*, *478*(1–2), 62–77, doi:10.1016/j.tecto.2009.03.013.

Ferraccioli, F., C. Finn, T. Jordan, R. Bell, L. Anderson, and D. Damaske (2011), East Antarctic rifting triggers uplift of the Gamburtsev Mountains, *Nature*, *479*(7373), 388–392, doi:10.1038/nature10566.

Fischer, H., et al. (2013), Where to find 1.5 million yr old ice for the IPICS "Oldest-Ice" ice core, *Clim. Past*, *9*(6), 2489–2505, doi:10.5194/cp-9-2489-2013.

Floberghagen, R., M. Fehringer, D. Lamarre, D. Muzi, B. Frommknecht, C. Steiger, J. Piñeiro, and A. da Costa (2011), Mission design, operation and exploitation of the gravity field and steady-state ocean circulation explorer mission, *J. Geod.*, *85*(11), 749–758, doi:10.1007/s00190-011-0498-3.

Forsberg, R. (1993), Modelling the fine-structure of the geoid: Methods, data requirements and some results, *Surv. Geophys.*, *14*, 403–418.

Forsberg, R., and C. Tscherning (1997), Topographic effects in gravity field modelling for BVP, in *Geodetic Boundary Value Problems in View of the One Centimeter Geoid, Lect. Notes Earth Sci.*, vol. 65, edited by F. Sansò and R. Rummel, pp. 241–272, Springer, Berlin.

Forsberg, R., and C. C. Tscherning (2008), *An Overview Manual for the GRAVSOFT Geodetic Gravity Field Modelling Programs*, 2nd ed., Danish Technical University and University of Copenhagen, Copenhagen.

Forsberg, R., M. G. Sideris, and C. K. Shum (2005), The gravity field and GGOS, *J. Geodyn.*, *40*(4–5), 387–393, doi:10.1016/j.jog.2005.06.014.

Förste, C., et al. (2014), EIGEN-6C4: The latest combined global gravity field model including GOCE data up to degree and order 2190 of GFZ Potsdam and GRGS Toulouse, paper presented at 5th GOCE User Workshop, Paris, 25–28 Nov.

Fretwell, P., et al. (2013), Bedmap2: Improved ice bed, surface and thickness datasets for Antarctica, *Cryosphere*, *7*(1), 375–393, doi:10.5194/tc-7-375-2013.

Golynsky, A., et al. (2013), Air and shipborne magnetic surveys of the Antarctic into the 21st century, *Tectonophysics*, *585*, 3–12, doi:10.1016/j.tecto.2012.02.017.

Hackney, R. I., and W. E. Featherstone (2003), Geodetic versus geophysical perspectives of the 'gravity anomaly', *Geophys. J. Int.*, *154*, 35–43.

Jokat, W., T. Boebel, M. König, and U. Meyer (2003), Timing and geometry of early Gondwana breakup, *J. Geophys. Res.*, *108*(B9), 2428, doi:10.1029/2002JB001802.

Jordan, T., F. Ferraccioli, D. Vaughan, J. Holt, H. Corr, D. Blankenship, and T. Diehl (2010), Aerogravity evidence for major crustal thinning under the Pine Island Glacier region (West Antarctica), *GSA Bull.*, *122*(5–6), 714–726, doi:10.1130/B26417.1.

Jordan, T., F. Ferraccioli, E. Armadillo, and E. Bozzo (2013a), Crustal architecture of the Wilkes Subglacial Basin in East Antarctica, as revealed from airborne gravity data, *Tectonophysics*, *585*, 196–206, doi:10.1016/j.tecto.2012.06.041.

Jordan, T., F. Ferraccioli, N. Ross, M. Siegert, H. Corr, P. Leat, R. Bingham, D. Rippin, and A. le Brocq (2013b), Inland extent of the Weddell Sea Rift imaged by new aerogeophysical data, *Tectonophysics*, *585*, 137–160, doi:10.1016/j.tecto.2012.09.010.

Kenyon, S., R. Forsberg, and B. Coakley (2008), New gravity field for the Arctic, *Eos Trans. AGU*, *89*(32), 289–290, doi:10.1029/2008EO320002.

Krupnik, I., I. Allison, R. Bell, P. Cutler, D. Hik, J. López-Martínez, V. Rachold, E. Sarukhanian, and C. Summerhayes (Eds.) (2011), *Understanding Earth's Polar Challenges: International Polar Year 2007–2008*, CCI Press pp., Edmonton, Alberta and University of the Arctic, Rovaniemi, Finland (printed version) and ICSU/WMO Joint Committee for International Polar Year 2007–2008.

Maule, C. F., M. E. Purucker, N. Olsen, and K. Mosegaard (2005), Heat flux anomalies in Antarctica revealed by satellite magnetic data, *Science*, *309*(5733), 464–467, doi:10.1126/science.1106888.

Mayer-Gürr, T. (2012), The new combined satellite only model GOCO03S, paper presented at GGHS 2012, Venice, Italy, 9–12 Oct.

Metzler, B., and R. Pail (2005), GOCE data processing: The spherical cap regularization approach, *Stud. Geophys. Geod.*, *49*(4), 441–462, doi:10.1007/s11200-005-0021-5.

Moritz, H. (1984), Geodetic reference system 1980, *Bull. Geod.*, *58*, 395–405, (J. Geod., 58(3), 388–398, doi:10.1007/BF02519014).

Näslund, J.-O. (2001), Landscape development in western and central Dronning Maud Land, East Antarctica, *Antarct. Sci.*, *13*(3), 302–311, doi:10.1017/S0954102001000438.

NIMA (2000), Department of Defense World Geodetic System 1984: Its definition and relationships with local geodetic systems, NIMA Tech. Rep. 8350.2, 3rd ed., foreword by W. M. Mularie, National Imagery and Mapping Agency, St. Louis, Mo.

O'Donnell, J. P., and A. A. Nyblade (2014), Antarctica's hypsometry and crustal thickness: Implications for the origin of anomalous topography in East Antarctica, *Earth Planet. Sci. Lett.*, *388*, 143–155, doi:10.1016/j.epsl.2013.11.051.

Pail, R., et al. (2010), Combined satellite gravity field model GOCO01S derived from GOCE and GRACE, *Geophys. Res. Lett.*, *37*, L20314, doi:10.1029/2010GL044906.

Pail, R., et al. (2011), First GOCE gravity field models derived by three different approaches, *J. Geod.*, *85*(11), 819–843, doi:10.1007/s00190-011-0467-x.

Pavlis, N. K., S. A. Holmes, S. C. Kenyon, and J. K. Factor (2008), An Earth gravitational model to degree 2160: EGM2008, paper presented at EGU General Assembly, Vienna, 13–18 Apr.

Riedel, S., and W. Jokat (2007), A compilation of new airborne magnetic and gravity data across Dronning Maud Land, Antarctica, Extended Abstract 149, in *Antarctica: A Keystone in a Changing World, Online Proc. 10th ISAES, USGS Open File Rep. 2007-1047*, edited by A. Cooper et al., 4 pp., United States Geological Survey, Reston, Va., doi:10.3133/of2007-1047.

Riedel, S., W. Jokat, and D. Steinhage (2012), Mapping tectonic provinces with airborne gravity and radar data in Dronning Maud Land, East Antarctica, *Geophys. J. Int.*, *189*(1), 414–427, doi:10.1111/j.1365-246X.2012.05363.x.

Rudenko, S., D. Dettmering, S. Esselborn, T. Schöne, C. Förste, J.-M. Lemoine, M. Ablain, D. Alexandre, and K.-H. Neumayer (2014), Influence of time variable geopotential models on precise orbits of altimetry satellites, global and regional mean sea level trends, *Adv. Space Res.*, *54*(1), 92–118, doi:10.1016/j.asr.2014.03.010.

Sandwell, D. T., R. D. Müller, W. H. F. Smith, E. Garcia, and R. Francis (2014), New global marine gravity model from CryoSat-2 and Jason-1 reveals buried tectonic structure, *Science*, *346*(6205), 65–67, doi:10.1126/science.1258213.

Sansò, F., and M. G. Sideris (Eds.) (2013), *Geoid determination—Theory and methods*,Springer, Berlin, doi:10.1007/978-3-540-74700-0.

Scheinert, M. (2012), Progress and prospects of the Antarctic Geoid Project (Commission Project 2.4), in *Geodesy for Planet Earth, Int. Assoc. Geodesy Symposia*, vol. 136, edited by S. Kenyon, M. C. Pacino, and U. Marti, pp. 451–456, Springer, Berlin, doi:10.1007/978-3-642-20338-1_54

Schroeder, D. M., D. D. Blankenship, D. A. Young, and E. Quartini (2014), Evidence for elevated and spatially variable geothermal flux beneath the West Antarctic Ice Sheet, *Proc. Natl. Acad. Sci. U.S.A.*, *111*(25), 9070–9072, doi:10.1073/pnas.1405184111.

Schwabe, J., and M. Scheinert (2014), Regional geoid of the Weddell Sea, Antarctica, from heterogeneous ground-based gravity data, *J. Geod.*, *88*(9), 821–838, doi:10.1007/s00190-014-0724-x.

Schwabe, J., M. Scheinert, R. Dietrich, F. Ferraccioli, and T. Jordan (2012), Regional geoid improvement over the Antarctic Peninsula utilizing airborne gravity data, in *Geodesy for Planet Earth, Int. Assoc. of Geodesy Symposia*, vol. 136, edited by S. Kenyon, M. C. Pacino, and U. Marti, pp. 457–464, Springer, Berlin, doi:10.1007/978-3-642-20338-1_55

Schwabe, J., H. Ewert, M. Scheinert, and R. Dietrich (2014), Regional geoid modeling in the area of subglacial Lake Vostok, Antarctica, *J. Geodyn.*, *75*, 9–21, doi:10.1016/j.jog.2013.12.002.

Shako, R., C. Förste, O. Abrikosov, S. Bruinsma, J.-C. Marty, J.-M. Lemoine, F. Flechtner, H. Neumayer, and C. Dahle (2014), EIGEN-6C: A high-resolution global gravity combination model including GOCE data, in *Observation of the System Earth From Space - CHAMP, GRACE, GOCE and Future Missions, Adv. Technol. in Earth Sci.*, edited by F. Flechtner, N. Sneeuw, and W.-D. Schuh, pp. 155–161, Springer, Berlin, doi:10.1007/978-3-642-32135-1-20

Smith, W. H. F., and P. Wessel (1990), Gridding with continuous curvature splines in tension, *Geophysics*, *55*, 293–305.

Stern, T. A., and U. S. ten Brink (1989), Flexural uplift of the transantarctic mountains, *J. Geophys. Res.*, *94*, 10,315–10,330.

Studinger, M. (1998), Compilation and analysis of potential field data from the Weddell Sea, Antarctica: Implications for the break-up of Gondwana, Berichte zur Polarforschung (Report on Polar Research) 276, Alfred Wegener Institute for Polar and Marine Research, Bremerhaven.

Studinger, M., R. Bell, W. Buck, G. Karner, and D. Blankenship (2004), Sub-ice geology inland of the transantarctic mountains in light of new aerogeophysical data, *Earth Planet. Sci. Lett.*, *220*, 391–408, doi:10.1016/S0012-821X(04)00066-4.

Studinger, M., R. E. Bell, P. G. Fitzgerald, and W. R. Buck (2006), Crustal architecture of the transantarctic mountains between the Scott and Reedy Glacier region and South Pole from aerogeophysical data, *Earth Planet. Sci. Lett.*, *250*(1–2), 182–199, doi:10.1016/j.epsl.2006.07.035.

Studinger, M., L. Koenig, S. Martin, and J. Sonntag (2010), Operation icebridge: Using instrumented aircraft to bridge the observational gap between IceSat and IceSat-2,paper presented at IEEE International Geoscience and Remote Sensing Symposium (IGARSS), 2010, pp. 1918–1919, Honolulu, Hawaii, 25–30 Jul., doi:10.1109/IGARSS.2010.5650555.

Tapley, B. D., S. Bettadpur, M. Watkins, and C. Reigber (2004), The gravity recovery and climate experiment: Mission overview and early results, *Geophys. Res. Lett.*, *31*, L09607, doi:10.1029/2004GL019920.

Tapley, B. D., F. Flechtner, S. V. Bettadpur, and M. M. Watkins (2014), The GRACE mission: Status and future activities, Abstract G23C-03 presented at 2014 Fall Meeting, AGU, San Francisco, Calif., 15–19 Dec.

van der Meijde, M., R. Pail, R. Bingham, and R. Floberghagen (2015), GOCE data, models, and applications: A review, *Int. J. Appl. Earth Obs. Geoinf.*, *35*, 4–15, doi:10.1016/j.jag.2013.10.001.
Watts, A. B. (2001), *Isostasy and Flexure of the Lithosphere*, Cambridge Univ. Press, 480 pp. pp., Cambridge, U. K.
Wessel, P., and W. H. F. Smith (2015), The Generic Mapping Tool GMT, Version 4.5.14, Technical Reference, Cookbook and Manpages.
Wessel, P., W. H. F. Smith, R. Scharroo, J. Luis, and F. Wobbe (2013), Generic mapping tools: Improved version released, *Eos Trans. AGU*, *94*(45), 409–410, doi:10.1002/2013EO450001.

Supporting Information for "New Antarctic Gravity Anomaly Grid for Enhanced Geodetic and Geophysical Studies in Antarctica"

M. Scheinert[1], F. Ferraccioli[2], J. Schwabe[1,12], R. Bell[3], M. Studinger[4], D. Damaske[5], W. Jokat[6,7], N. Aleshkova[8], T. Jordan[2], G. Leitchenkov[8,9], D. D. Blankenship[10], T. M. Damiani[11], D. Young[10], J. R. Cochran[3], T. D. Richter[10]

Contents of this file

Additional Supporting Information

1. Datasets are available at: http://dx.doi.org/10.1594/PANGAEA.848168.

Introduction

This supporting material provides additional background information to the main paper. Namely, we provide remarks on the history of AntGG (to complement Section 2 of the main text), a detailed explanation on the choice of the background earth gravity model (to complement Section 4 of the main text), and supplementing remarks on the remove-compute-restore technique (to complement Subsection 5.2 of the main text).

Figures S1 to S3 add more detailed views on the numbering and propagated RMS of the individual gravity datasets used in our continental-scale Antarctic gravity compilation (Fig. S1), on the number of overlapping datasets (Fig. S2) and on the RMS of residual individual datasets w.r.t. the residual gridded dataset (Fig. S3). For details, refer to Section 5 of the paper.

Table S1 is an extended version of Table 1 of the main paper, giving more detailed metadata such as survey line and tie line spacing of the airborne surveys, referred quantity (gravity anomaly Δg or gravity disturbance δg), used gravity formula, observation height levels, reference heights, height datum, and a priori standard deviation σ_0. Table S2 summarizes some statistics for the datasets (in addition to Section 5.3 of the main paper).

Figures S4 and S5 refer to Section S2 of this supporting information.

S1. Remarks on the history of AntGG (Supplement to Section 2)

In the framework of international organizations such as International Association of Geodesy (IAG) and Scientific Committee on Antarctic Research (SCAR) several attempts were started to overcome the deficient coverage of gravity data in Antarctica. An early IAG initiative dates back to 1993 [*Sjöberg and Fan*, 1993]. The SCAR Expert Group on Geodetic Infrastructure in Antarctica (GIANT) has defined an appropriate project in its work program (named "Gravity Field" since 2012). As one of the projects to compile Antarctic gravity data of different sources the Antarctic Digital Gravity Synthesis (ADGRAV) shall be mentioned which originated from an initiative of the SCAR Working Group on Solid Earth Geophysics in 1998 [*Bell*, 2000]. In 2003, IAG initiated a working group to deal with the issue which in 2011 was transferred to IAG Sub-Commission 2.4f "Gravity and Geoid in Antarctica" (AntGG), chaired by the first author [*Scheinert*, 2005; *Scheinert et al.*, 2008; *Scheinert*, 2011, 2012; *Scheinert et al.*, 2013].

S2. Choice of the background global Earth Gravity Model (Supplement to Section 4)

In order to investigate the performance of recent Earth Gravity Models (EGM) over Antarctica, a comparison was carried out using high-resolution ground-based airborne gravity datasets that can be regarded as providing ground truth for these global models. To demonstrate that the global EGMs yield different predictions depending on whether the respective region is located *inside* or *outside* the polar data gap resulting from the GOCE orbit inclination (see Section 3), two datasets were chosen accordingly. A better performance would be expected adopting a dataset outside the polar data gap. Comparing the EGM with a dataset inside the polar data gap, on the other hand, the effects of satellite data deficiency and of the respective regularization technique should become visible. Latest ESA GOCE-based models, the latest ITSG GRACE model [*Mayer-Gürr*

[1]Institut für Planetare Geodäsie, Technische Universität Dresden, Dresden, Germany.
[2]British Antarctic Survey, High Cross, Madingley Road, Cambridge, UK.
[3]Lamont-Doherty Earth Observatory of Columbia University, Palisades, NY, USA.
[4]NASA Goddard Space Flight Center, MD, USA.
[5]Bundesanstalt für Geowissenschaften und Rohstoffe, Hannover, Germany.
[6]Alfred-Wegener-Institut, Helmholtz-Zentrum für Polar- und Meeresforschung, Bremerhaven, Germany.
[7]University of Bremen, Geoscience Department, Bremen, Germany.
[8]VNIIOkeangeologia, St. Petersburg, Russia.
[9]St. Petersburg State University, St. Petersburg, Russia.
[10]Institute for Geophysics, Jackson School of Geosciences, University of Texas at Austin, TX, USA.
[11]National Geodetic Survey, NOAA, Silver Spring, MD, USA.
[12]now at: Bundesamt für Kartographie and Geodäsie, Leipzig, Germany.

0094-8276/16/$5.00

et al., 2014] and two combined EGMs were used to compute gravity disturbances at flight altitude which were then subtracted from the respective airborne data. The truncation degree of the harmonic series expansion was stepwise increased by one up to the maximum degree 300. Thus, we obtained differences for each EGM at each truncation degree, that is given at the axis of abscissae in Figures S4 and S5. These differences, which can be considered as residual gravity disturbances, contain the omission error (due to truncation of the harmonic expansion at the respective degree) and the commission error of the EGM (due to the propagation of measurement errors into the model solution) as well as the error noise of the airborne measurements. From the residual gravity disturbances *mean difference, standard deviation* and *maximum absolute difference* were calculated and plotted over the respective truncation degree (Figures S4 and S5). These three parameters were used to evaluate the performance of the different EGMs.

S2.1. Lake Vostok survey

Outside the polar data gap, the Lake Vostok (LVS) survey [*Studinger et al.*, 2003a, b; *Holt et al.*, 2006] provided a homogeneous, high-quality dataset. It covered an area of approx. 165 by 330 km (dataset #16, for location see Fig. S1, for metadata see Tab. S1), thus capturing a maximum half-wavelength of 165 km which corresponds to approx. d/o 155. Therefore, a spectral gap should not occur in the residual data. The residual gravity disturbances were taken at the reference altitude of 3,960 m.

Figure S4 shows the three parameters determined from the residual gravity disturbances as described above. The mean differences (Fig. S4, top panel) of almost all models exhibit a quite uniform behavior. They converge in a band of ±1 mGal, that is below the reported a priori accuracy of the airborne gravity data, and remain almost constant from approx. d/o 210 onwards. Therefore, both EGM and airborne data can be regarded unbiased. However, the mean differences also indicate that GOCO03S [*Mayer-Gürr*, 2012] coincides best with the airborne data. Over the Antarctic continent the combined model EGM2008 [*Pavlis et al.*, 2008] does not contain additional information apart from GRACE observations up to d/o 180. Therefore, its mean difference remains constant at about –6 mGal above that d/o. Unlike EGM2008, EIGEN-6C4 [*Förste et al.*, 2014] also incorporates GOCE observations. It fits slightly better, but is also degraded compared to the satellite-only model EIGEN-6S2 [*Rudenko et al.*, 2014] due to missing terrestrial data.

A similar behavior can be noted for the standard deviations (Fig. S4, middle panel). From d/o 170 EGM2008 remains on a level of about 35 mGal, likewise EIGEN-6C4 (level of about 33 mGal above d/o 200). ITSG-Grace2014 [*Mayer-Gürr et al.*, 2014] shows peculiar oscillations starting at about d/o 180, i.e., close to its formal maximum d/o 200. The fact, that ITSG-Grace2014 was inferred without applying any (Kaula-type) constraint could explain this behavior. This is in accordance with its signal-to-noise ratio falling below one at d/o 170 to 180 [ibid]. The lowest standard deviation approximating the airborne data in that region is obtained for the ESA timewise and direct models ESA-TIM/R5 and ESA-DIR/R5 (better than 25 mGal above d/o 240). GOCO03S, EIGEN-6S2 and ESA's spacewise model ESA-SPW/R4 perform only slightly worse (27 mGal from d/o 220). Similar properties can be stated in terms of the maximum absolute difference (Fig. S4, lower panel).

S2.2. Pensacola Pole Transect survey

To deal with terrestrial gravity data inside the polar data gap of GOCE there are not many surveys to chose from. The Pensacola Pole Transect (PPT) survey was selected [*Davis*, 2001; *Studinger et al.*, 2006] (dataset #14, for location see Fig. S1, for metadata see Table S1), because it provided the only dataset which is almost completely situated inside the polar data gap. It covered a narrow strip of 100 by 800 km and was flown at different altitudes, starting at 800 m close to the southern tip of the Ross Ice Shelf and covering a range of 3,150 to 3,700 m over the Antarctic ice sheet.

The three parameters obtained to characterize the resulting residual gravity disturbances (Figure S5) reveal a strikingly different behavior. In the mean difference (Fig. S5, top panel), a considerable bias is visible. Except ITSG-Grace2014 all models remain at a stable level between 28 and 35 mGal above d/o 210 with ESA-TIM/R5 showing the lowest bias and GOCO03S the largest bias. One could discuss if this bias reveals a spectral gap caused by an inconsistency between the EGM resolution and the extension of the area covered by the airborne survey. However, the mean difference of all EGM remains almost constant above d/o 210. Therefore, most likely there is a bias in the airborne data.

The standard deviations of the residual gravity disturbances (Fig. S5, middle panel) are even more meaningful. In contrast to the Lake Vostok case the combined models EGM2008 and EIGEN-6C4 provide the best representation inside the polar data gap. However, their standard deviations are not much better than those of ESA's direct model ESA-DIR/R5 and, up to their maximum d/o, of GOCO03S and EIGEN-6S2. This is due to the fact that no additional information went into the spherical harmonic solution up to d/o 250. The ESA spacewise and timewise models (ESA-SPW/R4 and ESA-TIM/R5) are performing worse (level of 26 mGal compared to 20 to 21 mGal for the other models). Thus, the stabilizing effect becomes visible, either of the spherical cap regularization (ESA-DIR/R5) or of the GRACE data that were incorporated into the combination (EIGEN-6S2 and GOCO03S). Again, this is no surprise since GOCE is not sensitive at the longer wavelengths (cf. above). The model ISTG-Grace2014 exhibits larger oscillations similar to the case of the Lake Vostok survey due to their unconstrained inference. Most interestingly, the lower panel of Fig. S5 reveals that the GOCO03S model provides by far smaller maximum residuals, i.e. a much smoother representation inside the polar data gap. This holds true even at the highest resolution.

S2.3. Conclusion

The investigation of global EGMs was focused on the Antarctic continent, since a different picture can be expected when considering regions close to the pole or even inside the polar data gap caused by GOCE's inclination. The comparison was done in terms of residual gravity disturbances, taken a respective maximum degree of the harmonic expansion of the EGMs. From the comparison with the Lake Vostok survey (dataset #16) – outside the polar data gap – one can conclude that GOCO03S does not perform worse than the latest ESA GOCE models ESA-DIR/R5 and ESA-TIM/R5. Comparing the models with the Pensacola Pole Transect survey (dataset #14) – situated inside the polar data gap –, from the mean difference one cannot conclude which model performs best. Instead, most likely there is a bias in the airborne data. On the other hand, in the standard deviation as well as in the mean difference it becomes visible whether GRACE data were used (or not used) in the determination of the model in order to mitigate the polar data gap problem. In the determination of the ESA-TIM/R5 model, GRACE observations were not introduced. In the determination of GOCO03S and ESA-DIR/R5, GOCE data were

combined with GRACE data. For all three models an additional regularization technique was applied (either Kaulas rule of thumb using synthetic degree variances or the spherical cap regularization according to *Metzler and Pail* [2005]). It becomes clear that the inclusion of GRACE data is superior, since ESA-TIM/R5 performs worse than GOCO03S and ESA-DIR/R5 (especially in terms of the maximum absolute difference). Thus, ESA-DIR/R5 and ESA-TIM/R5 might generally be better in terms of accuracy and spatial resolution, but only if one investigates these models over the entire globe. If emphasis is put on the Antarctic continent alone, the results are different as shown by our evaluation.

Altogether, one can state that the GOCO03S model [*Mayer-Gürr*, 2012] utilizes the GOCE observations in an appropriate way with minimum degradation of signals including the interior of the polar gap (which is due to the inclusion of GRACE data). The latest GOCE-based models have improved compared to earlier versions but still do not appear to perform better than GOCO03S. Therefore, it is an appropriate choice to apply GOCO03S as a background EGM to serve as the common reference in adjusting the terrestrial Antarctic gravity datasets.

S3. Short description of publicly available datasets

Datasets are available at: http://dx.doi.org/10.1594/PANGAEA.848168.

We provide the data in two different formats, namely ASCII and NetCDF, respectively. Grid coordinates x and y are given according to polar stereographic projection, projection centre at 90°S, true scale at 71°S, ellipsoid WGS84, unit: km. Longitude and latitude of the grid points are calculated according to the inverse polar stereographic projection. Subsequently, all data are also given as functions of (x, y), namely:

– Ellipsoidal surface height [m] from Bedmap2 [*Fretwell et al.*, 2013]; in area north of 60°S values are set to *NaN*;

– Orthometric surface height [m] from Bedmap2 [*Fretwell et al.*, 2013]; in area north of 60°S values are set to zero (corresponding to sea level);

– Free-air gravity anomaly [mGal] at surface (Fig. 1 of main paper);

– Accuracy measure [mGal] for the free-air gravity anomaly (RMS, propagated from a priori standard deviation) (Fig. S3);

– Complete Bouguer anomaly [mGal] (Fig. 2 of main paper).

References

Aitken, A. R. A., D. A. Young, F. Ferraccioli, P. G. Betts, J. S. Greenbaum, T. G. Richter, J. L. Roberts, D. D. Blankenship, and M. J. Siegert (2014), The subglacial geology of Wilkes Land, East Antarctica, *Geophys. Res. Lett.*, *41*(7), 2390–2400, doi: 10.1002/2014GL059405.

Aleshkova, N., A. Golynsky, R. Kurinin, and V. Mandrikov (2000a), Gravity mapping in the southern Weddell Sea region, *Polarforschung*, *67*(3), 91–99, (1997, published 2000).

Aleshkova, N., A. Golynsky, R. Kurinin, and V. Mandrikov (2000b), Gravity Mapping in the Southern Weddell Sea Region. (Explanatory note for free-air and Bouguer anomalies maps), *Polarforschung*, *67*(3), 163–177, (1997, published 2000).

Aleshkova, N., V. Masolov, G. Leitchenkov, V. Mandrikov, S. Alyavdin, A. Golynsky, and R. Kurinin (2004), Russian Antarctic Gravity Dataset, Poster presentation at SCAR XXVIII Open Science Conference, Bremen, July 26-28, 2004.

Bell, R. (2000), Antarctic Digital Gravity Synthesis (ADGRAV), data compilation 1990-2000, Lamont-Doherty Earth Observatory, Columbia University, http://www.marine-geo.org/tools/search/entry.php?id=ADGRAV (last accessed: 03 Feb 2015).

Bell, R., J. Brozena, W. Haxby, and J. LaBrecque (1990), Continental margins of the western Weddell Sea: insights from airborne gravity and GEOSAT-derived gravity, in *Contributions to Antarctic Research*, *Antarctic Research Series*, vol. 50, edited by D. Elliott, pp. 91–102, American Geophys. Union.

Bell, R. E., V. A. Childers, R. A. Arko, D. D. Blankenship, and J. M. Brozena (1999), Airborne gravity and precise positioning for geologic applications, *J. Geophys. Res.*, *104*(B7), 15,281–15,292, doi:10.1029/1999JB900122.

Brozena, J., J. LaBreque, M. Peters, R. Bell, and C. Raymond (1990), Airborne Gravity Measurement over Sea-Ice: The Western Weddell Sea, *Geophys. Res. Lett.*, *17*(11), 1941–1944, doi: 10.1029/GL017i011p01941.

Cochran, J. R., and R. E. Bell (2012), Inversion of IceBridge gravity data for continental shelf bathymetry beneath the Larsen Ice Shelf, Antarctica, *J. Glac.*, *58*(209), 540–552, doi: 10.3189/2012JoG11J033.

Damaske, D., and M. McLean (2005), An Aerogeophysical Survey South of the Prince Charles Mountains, East Antarctica, *Terra Antarctica*, *12*(2), 87–98.

Davis, M. (2001), Subglacial Morphology and Structural Geology in the Southern Transantarctic Mountains from Airborne Geophysics, M.S. Thesis, University of Texas, 133pp.

Diehl, T., J. Holt, D. Blankenship, D. Young, T. Jordan, and F. Ferraccioli (2008), First airborne gravity results over the Thwaites Glacier catchment, West Antarctica, *Geochem. Geophys. Geosyst.*, *9*(4), doi:10.1029/2007GC001878.

Ferraccioli, F., P. Jones, M. Curtis, and P. Leat (2005), Subglacial imprints of early Gondwana break-up as identified from high resolution aerogeophysical data over western Dronning Maud Land, East Antarctica, *Terra Nova*, *17*, 573–579, doi: 10.1111/j.1365-3121.2005.00651.x.

Ferraccioli, F., P. Jones, A. Vaughan, and P. Leat (2006), New aerogeophysical view of the Antarctic Peninsula: More pieces, less puzzle, *Geophys. Res. Lett.*, *33*, L05,310, doi: 10.1029/2005GL024636.

Ferraccioli, F., C. Finn, T. Jordan, R. Bell, L. Anderson, and D. Damaske (2011), East Antarctic rifting triggers uplift of the Gamburtsev Mountains, *Nature*, *479*(7373), 388–392, doi: 10.1038/nature10566.

Ferris, J. K., B. C. Storey, A. P. M. Vaughan, P. R. Kyle, and P. C. Jones (2003), The Dufek and Forrestal intrusions, Antarctica: A centre for Ferrar Large Igneous Province dike emplacement?, *Geophys. Res. Lett.*, *30*(6), doi: 10.1029/2002GL016719.

Förste, C., et al. (2014), EIGEN-6C4: The latest combined global gravity field model including GOCE data up to degree and order 2190 of GFZ Potsdam and GRGS Toulouse, pres., 5th GOCE User Workshop, Paris, 25-28 Nov 2014.

Fretwell, P., et al. (2013), Bedmap2: improved ice bed, surface and thickness datasets for Antarctica, *The Cryosphere*, *7*(1), 375–393, doi: 10.5194/tc-7-375-2013.

Greischar, L. L., C. R. Bentley, and L. R. Whiting (1992), An Analysis of Gravity Measurements on the Ross Ice Shelf, Antarctica, in *Contributions to Antarctic Research III*, *Antarctic Research Series*, vol. 57, edited by D. H. Elliot, pp. 105–155, American Geophys. Union.

Herrod, L. (1987), A geophysical reconnaissance of Ronne Ice Shelf, Antarctica, PhD thesis, University of Cambridge.

Holt, J., T. Richter, S. Kempf, D. Morse, and D. Blankenship (2006), Airborne gravity over Lake Vostok and adjacent highlands of East Antarctica, *Geochem. Geophys. Geosyst.*, *7*(11), 15, doi:10.1029/2005GC001177.

Jones, P., A. Johnson, R. v. Frese, and H. Corr (2002), Detecting rift basins in the Evans Ice Stream region of West Antarctica using airborne gravity data, *Tectonophys.*, *347*, 25–41.

Jordan, T., F. Ferraccioli, P. Jones, J. Smellie, M. Ghidella, and H. Corr (2009), Airborne gravity reveals interior of Antarctic volcano, *Phys. Earth Plan. Int.*, *175*(3-4), 127–136, doi: 10.1016/j.pepi.2009.03.004.

Jordan, T., F. Ferraccioli, D. Vaughan, J. Holt, H. Corr, D. Blankenship, and T. Diehl (2010), Aerogravity evidence for major crustal thinning under the Pine Island Glacier region (West Antarctica), *GSA Bulletin*, *122*(5-6), 714–726, doi: 10.1130/B26417.1.

Jordan, T., F. Ferraccioli, N. Ross, M. Siegert, H. Corr, P. Leat, R. Bingham, D. Rippin, and A. le Brocq (2013a), Inland extent of the Weddell Sea Rift imaged by new aerogeophysical data, *Tectonophys.*, *585*, 137–160, doi: 10.1016/j.tecto.2012.09.010.

Jordan, T., F. Ferraccioli, E. Armadillo, and E. Bozzo (2013b), Crustal architecture of the Wilkes Subglacial Basin in East Antarctica, as revealed from airborne gravity data, *Tectonophys.*, *585*, 196–206, doi: 10.1016/j.tecto.2012.06.041.

Karner, G. D., M. Studinger, and R. E. Bell (2005), Gravity anomalies of sedimentary basins and their mechanical implications: Application to the Ross Sea basins, West Antarctica, *Earth Plan. Sci. Lett.*, *235*, 577–596, doi:10.1016/j.epsl.2005.04.016.

Korth, W. (1998), Bestimmung von Oberflächengeometrie, Punktbewegungen und Geoid in einer Region der Antarktis, PhD Thesis, Deutsche Geodätische Kommission, C505, München.

LaBrecque, J., and M. Ghidella (1997), Bathymetry, depth to magnetic basement, and sediment thickness estimates from aerogeophysical data over the western Weddell Basin, *J. Geophys. Res.*, *102*(B4), 7929–7945.

Luyendyk, B., D. Wilson, and C. Siddoway (2003), Eastern margin of the Ross Sea Rift in western Marie Byrd Land, Antarctica: Crustal structure and tectonic development, *Geochem. Geophys. Geosyst.*, *4*(10), doi:10.1029/2002GC000462.

Maslanyi, M. (1991), Geophysical investigation of George VI Sound, Antarctic Peninsula, in *Geological Evolution of Antarctica*, edited by M. Thomson, J. Crame, and J. Thomson, pp. 527–530, Cambridge University Press.

Mayer-Gürr, T. (2012), The new combined satellite only model GOCO03S, presentation at GGHS 2012, Venice, October 2012.

Mayer-Gürr, T., N. Zehentner, B. Klinger, and A. Kvas (2014), ITSG-Grace2014: A new GRACE gravity field release computed in Graz, presentation at Grace Science Team Meeting, Potsdam, 29 Sept - 01 Oct. 2014.

McGibbon, K., and A. Smith (1991), New Geophysical results and preliminary interpretation of crustal structure between the Antarctic Peninsula and Ellsworth Land, in *Geological Evolution of Antarctica*, edited by M. Thomson, J. Crame, and J. Thomson, pp. 475–479, Cambridge University Press.

McLean, M., and G. Reitmayr (2005), An Airborne Gravity Survey South of the Prince Charles Mountains, East Antarctica, *Terra Antarctica*, *12*(2), 99–108.

Metzler, B., and R. Pail (2005), GOCE Data Processing: The Spherical Cap Regularization Approach, *Stud. Geophysica et Geodaetica*, *49*(4), 441–462, doi: 10.1007/s11200-005-0021-5.

Mieth, M., and W. Jokat (2014), New aeromagnetic view of the geological fabric of southern Dronning Maud Land and Coats Land, East Antarctica, *Gondwana Res.*, *25*, 358–367, doi: 10.1016/j.gr.2013.04.003.

Pavlis, N. K., S. A. Holmes, S. C. Kenyon, and J. K. Factor (2008), An Earth Gravitational Model to Degree 2160: EGM2008, presentation at EGU General Assembly, Vienna, April 13-18, 2008.

Reitmayr, G. (2005), Gravity Survey in Central Dronning Maud Land, East Antarctica, during the 1995/96 GeoMaud Expedition, in *International GEOMAUD Expedition of the BGR to Central Dronning Maud Land in 1995/96, Vol. II: Geophysical Results*, edited by H.-J. Paech, no. B97 in Geolog. Jahrbuch, pp. 141–164, Bundesanstalt für Geowissenschaften und Rohstoffe, Hannover.

Renner, R., L. Sturgeon, and S. Garrett (1985), Reconnaissance gravity and aeromagnetic surveys of the Antarctic Peninsula, in *Scientific Reports*, vol. 134, British Antarctic Survey.

Riedel, S., and W. Jokat (2007), A compilation of new airborne magnetic and gravity data across Dronning Maud Land, Antarctica, in *Antarctica: A Keystone in a Changing World, Online Proc. 10th ISAES, USGS Open-File Report*, edited by A. Cooper, C. Raymond, M. Diggles, and S. Mautner, doi: 10.3133/of2007-1047.ea149.

Riedel, S., W. Jokat, and D. Steinhage (2012), Mapping tectonic provinces with airborne gravity and radar data in Dronning Maud Land, East Antarctica, *Geophys. J. Int.*, *189*(1), 414–427, doi: 10.1111/j.1365-246X.2012.05363.x.

Riedel, S., J. Jacobs, and W. Jokat (2013), Interpretation of new regional aeromagnetic data over Dronning Maud Land (East Antarctica), *Tectonophys.*, *585*, 161–171, doi: 10.1016/j.tecto.2012.10.011.

Rudenko, S., D. Dettmering, S. Esselborn, T. Schöne, C. Förste, J.-M. Lemoine, M. Ablain, D. Alexandre, and K.-H. Neumayer (2014), Influence of time variable geopotential models on precise orbits of altimetry satellites, global and regional mean sea level trends, *Adv. Space Res.*, *54*(1), 92–118, doi: 10.1016/j.asr.2014.03.010.

Scheinert, M. (2005), The Antarctic Geoid Project: Status Report and Next Activities, in *Gravity, Geoid and Space Missions*, *International Association of Geodesy Symposia*, vol. 129, edited by C. Jekeli, L. Bastos, and J. Fernandes, pp. 137–142, Springer, Berlin - Heidelberg - New York, doi: 10.1007/3-540-26932-0_24.

Scheinert, M. (2011), Towards an improved knowledge of the gravity field and geoid in Antarctica utilizing airborne gravimetry, abstract G12A-05 presented at 2011 Fall Meeting, AGU, San Francisco, CA, 5-9 Dec 2011.

Scheinert, M. (2012), Progress and prospects of the Antarctic Geoid Project (Commission Project 2.4), in *Geodesy for Planet Earth*, *International Association of Geodesy Symposia*, vol. 136, edited by S. Kenyon, M. Pacino, and U. Marti, pp. 451–456, Springer Berlin Heidelberg, doi: 10.1007/978-3-642-20338-1_54.

Scheinert, M., J. Müller, R. Dietrich, D. Damaske, and V. Damm (2008), Regional Geoid Determination in Antarctica Utilizing Airborne Gravity and Topography Data, *J. Geod.*, *82*(7), 403–414, doi: 10.1007/s00190-007-0189-2.

Scheinert, M., S. Petrovic, I. Heyde, F. Barthelmes, J. Schwabe, C. Förste, and L. Eberlein (2013), From Germany to Antarctica: Airborne geodesy and geophysics and the utilization of the research aircraft HALO, abstract G13C-05 presented at 2013 Fall Meeting, AGU, San Francisco, CA, 9-13 Dec 2013.

Sjöberg, L. E., and H. Fan (1993), The Antarctic Gravity and Geoid Solution, report to the IAG General Meeting 1993, Beijing (unpublished).

Studinger, M. (1998), Compilation and analysis of potential field data from the Weddell Sea, Antarctica: Implications for the break-up of Gondwana, *Berichte zur Polarforschung (Reports on Polar Research) 276*, Alfred Wegener Institute for Polar and Marine Research, Bremerhaven.

Studinger, M., and H. Miller (1999), Crustal structure of the Filchner-Ronne Shelf and Coats Land, Antarctica, from gravity and magnetic data: Implications for the breakup of Gondwana, *J. Geophys. Res.: Solid Earth*, *104*(B9), 20,379–20,394, doi: 10.1029/1999JB900117.

Studinger, M., R. Bell, C. Finn, and D. Blankenship (2002), Mesozoic and Cenozoic extensional tectonics of the West Antarctic Rift System from high-resolution airborne geophysical mapping, *Roy. Soc. of New Zealand Bull.*, *35*, 563–569.

Studinger, M., et al. (2003a), Ice cover, landscape setting, and geological framework of Lake Vostok, East Antarctica, *Earth Planet. Sci. Lett.*, *205*(3-4), 195–210, doi: 10.1016/S0012-821X(02)01041-5.

Studinger, M., G. Karner, R. Bell, V. Levin, C. Raymond, and A. Tikku (2003b), Geophysical models for the tectonic framework of the Lake Vostok region, East Antarctica, *Earth Planet. Sci. Lett.*, *216*(4), 663–677, doi: 10.1016/S0012-821X(03)00548-X.

Studinger, M., R. Bell, W. Buck, G. Karner, and D. Blankenship (2004), Sub-ice geology inland of the Transantarctic Mountains in light of new aerogeophysical data, *Earth Planet. Sci. Lett.*, *220*, 391–408, doi:10.1016/S0012-821X(04)00066-4.

Studinger, M., R. E. Bell, P. G. Fitzgerald, and W. R. Buck (2006), Crustal architecture of the Transantarctic Mountains between the Scott and Reedy Glacier region and South Pole from aerogeophysical data, *Earth Plan. Sci. Lett.*, *250*(1–2), 182 – 199, doi: 10.1016/j.epsl.2006.07.035.

Studinger, M., L. Koenig, S. Martin, and J. Sonntag (2010), Operation IceBridge: Using instrumented aircraft to bridge the observational gap between IceSat and IceSat-2, *IEEE International*, pp. 1918–1919, doi:10.1109/IGARSS.2010.5650555, Geoscience and Remote Sensing Symposium (IGARSS) 2010.

Corresponding author: M. Scheinert, Technische Universität Dresden, Institut für Planetare Geodäsie, 01062 Dresden, Germany. (Mirko.Scheinert@tu-dresden.de)

Table S1. Summary of gravity datasets and available metadata. *Methods:* A: aerograv., G: ground-based relative grav., S: shipborne grav. n/a: not available or unknown. *Line km:* Total length of airborne profiles. *Spacing:* Separation of main lines / tie lines (where given). σ_0: A priori standard deviation (italic typed numbers: assumed values, see Sect. 5.1).

No	Campaign	Reference	Meth.	Line km	Spacing	Quantity	gravity formula	obs. height level(s) [m]	reference height [m]	height datum	σ_0 [mGal]
1	BAS-1996		A	(4,500)		δg	GRS80	2270–3890	2777	WGS84	*3.0*
2	BAS-Evans	*Jones et al.* [2002]	A	11,500	12	δg	GRS80	1340–2170	2777	WGS84	5.0
3	BAS-SPARC	*Ferraccioli et al.* [2006]	A	>20,000	5/25	δg	GRS80	2730–5350	2777	WGS84	3.0
4	BAS-AGAP	*Ferraccioli et al.* [2011]	A	120,000	5/33	δg	GRS80		in situ	WGS84	*3.0*
5	BAS-BBAS	*Jordan et al.* [2010]	A	30,000	30/30	δg	GRS80		in situ	WGS84	2.8
6	BAS-Dufek	*Ferris et al.* [2003]	A, G	8,300	5/20	δg	GRS80		in situ	WGS84	*3.0*
7	BAS-I&M AFI	*Jordan et al.* [2013a]	A	23,000	7.5/25	δg	GRS80		in situ	WGS84	*3.0*
8	BAS-JRI	*Jordan et al.* [2009]	A	3,500	2/10	δg	GRS80		in situ	WGS84	2.9
9	BAS-MAMOG	*Ferraccioli et al.* [2005]	A	15,500	1/8	δg	GRS80		in situ	WGS84	2.0
10	BAS-Torus	(unpublished)	A	(10,000)		δg	GRS80		in situ	WGS84	*3.0*
11	BAS-WLK	*Jordan et al.* [2013b]	A	(40,000)	8.8/44	δg	GRS80		in situ	WGS84	2.8
12	SOAR-WAIS	*Bell et al.* [1999]; *Studinger et al.* [2002]	A	150,000	5/5	δg	GRS80	varying	in situ	WGS84	3.0
13	SOAR-WMB	*Luyendyk et al.* [2003]	A	35,000	5.3–10.6	δg	GRS80	900–2300	in situ	WGS84	5.0
14	SOAR-PPT	*Davis* [2001]; *Studinger et al.* [2006]	A	13,000	10/30	δg	GRS80	800/3150/ 3400/3700	in situ	WGS84	*3.0*
15	SOAR-WLK	*Studinger et al.* [2004]	A	21,000	10.6/31.8	δg	GRS80	3050/3720/ 3850	in situ	WGS84	2.6
16	SOAR-LVS	*Studinger et al.* [2003a, b]; *Holt et al.* [2006]	A	20,000	7.5/11.25	δg	GRS80	3960	3960	WGS84	1.2
17	AGASEA	*Diehl et al.* [2008]	A	(38,000)	15/15	δg	GRS80	varying	3600	WGS84	2.3
18	ICECAP	*Aitken et al.* [2014]	A	(37,000)		δg	GRS80	varying	in situ	WGS84	*3.0*
19	PCMEGA	*Damaske and McLean* [2005]; *McLean and Reitmayr* [2005]	A	20,500	5/25	δg	GRS67	2160/2760/ 3360	in situ	WGS84	*3.0*
20	VISA	*Riedel and Jokat* [2007]; *Riedel et al.* [2012, 2013]; *Mieth and Jokat* [2014]	A	85,000	10–20	δg	GRS80	1200–4580	in situ	WGS84	4.0
21	USAC	*Bell et al.* [1990]; *Brozena et al.* [1990]; *LaBrecque and Ghidella* [1997]	A	(11,000)	35/35	δg	GRS80	260–870	in situ	WGS84	*3.0*
22	ICEBRIDGE	*Studinger et al.* [2010]; *Cochran and Bell* [2012]	A	>150,000		δg	GRS80	360–11550	in situ	WGS84	*3.0*
23	ADGRAV-ROSS	*Greischar et al.* [1992]; *Karner et al.* [2005]	G			Δg	n/a	varying	n/a	n/a	*5.0*
24	GEOMAUD	*Korth* [1998]; *Reitmayr* [2005]	G			δg	GRS80	50–3090	in situ	WGS84	*1.0*
25	BAS-LAND	*Renner et al.* [1985]; *Herrod* [1987]; *Maslanyi* [1991]; *McGibbon and Smith* [1991]	G			Δg	GRS80	0–2660	in situ	n/a	*20*
26	PMGE/VNIIO	*Studinger* [1998]; *Studinger and Miller* [1999]; *Aleshkova et al.* [2000a, b, 2004]	A,G,S	190,000	20/50/100	n/a	GRS67	varying	n/a	n/a	10
27	ADGRAV-AWI		S			Δg	GRS80	0	in situ	MSL	*2.0*

Table S2. Statistics of gridded residual gravity anomalies $[\delta(\Delta g)^{(i)}]$ after subtraction of background EGM (remove step) and grid interpolation (compute step/project). Values are given in mGal.

No	Campaign	Mean	Standard Deviation
1	BAS-1996	-1.0	34.8
2	BAS-Evans	5.0	28.8
3	BAS-SPARC	3.3	27.7
4	BAS-AGAP	1.2	16.9
5	BAS-BBAS	0.3	15.1
6	BAS-Dufek	22.2	39.8
7	BAS-I&M AFI	-3.9	20.8
8	BAS-JRI	1.7	27.2
9	BAS-MAMOG	8.3	38.8
10	BAS-Torus	-7.4	28.5
11	BAS-WLK	5.0	22.4
12	SOAR-WAIS	40.9	16.3
13	SOAR-WMB	25.2	18.2
14	SOAR-PPT	34.4	21.2
15	SOAR-WLK	-13.4	16.9
16	SOAR-LVS	0.6	25.8
17	AGASEA	0.5	15.9
18	ICECAP	0.7	19.4
19	PCMEGA	-1.0	29.4
20	VISA	8.8	23.8
21	USAC	0.0	11.6
22	ICEBRIDGE	-0.8	16.8
23	ADGRAV-ROSS	6.7	31.2
24	GEOMAUD	-0.7	23.3
25	BAS-LAND	26.4	41.3
26	PMGE/VNIIO	4.5	17.0
27	ADGRAV-AWI	10.5	13.0

Table S3. Statistics of derived free-air gravity anomaly Δg, complete Bouguer anomaly Δg_B and, for comparison, simple Bouguer anomaly Δg_{plate} (only plate reduction applied).

Dataset / Parameter	Mean	Standard Deviation	RMS	Minimum	Maximum
Free-air anomaly Δg	-0.48	32.92	32.92	-384.49	204.84
Complete Bouguer anomaly Δg_B	48.06	154.16	161.48	-395.63	371.92
Simple Bouguer anomaly Δg_{plate}	50.73	165.55	173.15	-430.06	399.26

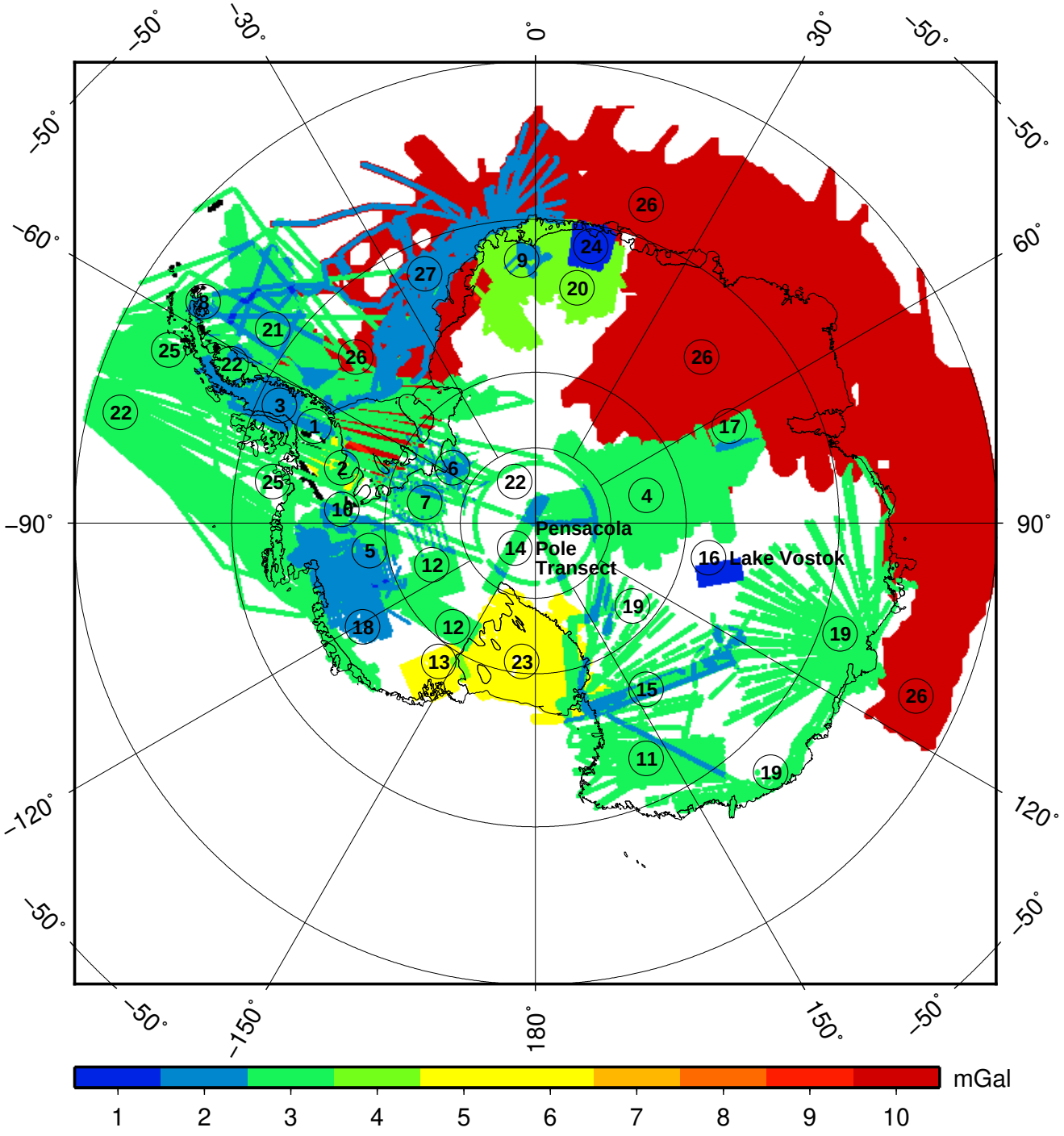

Figure S1. RMS propagated from a priori standard deviations in the process of interpolation and calculation of weighted mean. The RMS can be taken as an accuracy measure using the gravity anomalies for further analyses. Also, this map shows the extension of the different datasets and their overlapping. Numbers denote individual datasets (cf. Table S1). Additionally, the datasets are explicitely designated which were used for the investigation in Section S2, namely dataset #14 (Pensacola Pole Transect) and dataset #15 (Lake Vostok).

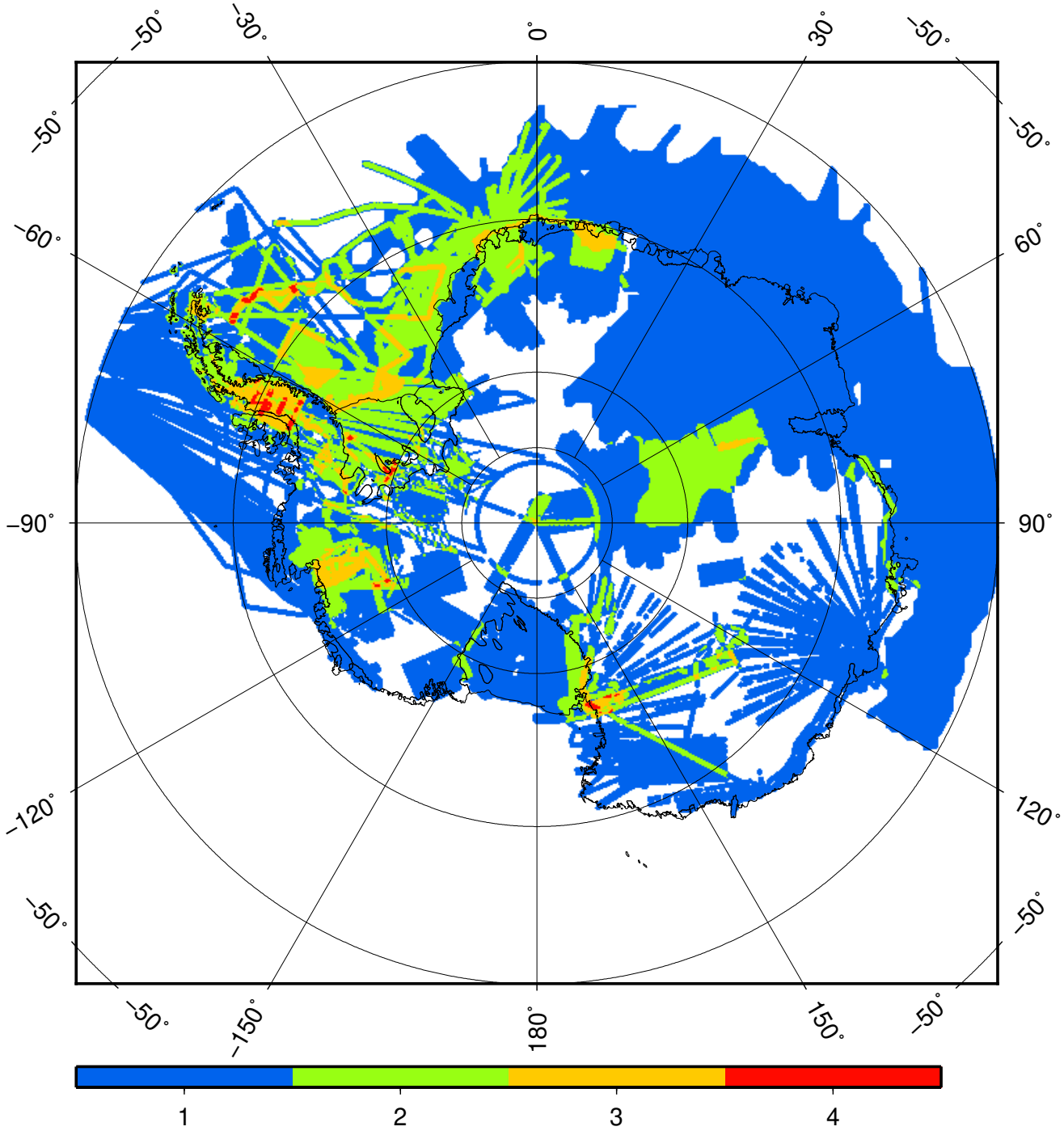

Figure S2. Number of datasets overlapping in certain areas in Antarctica.

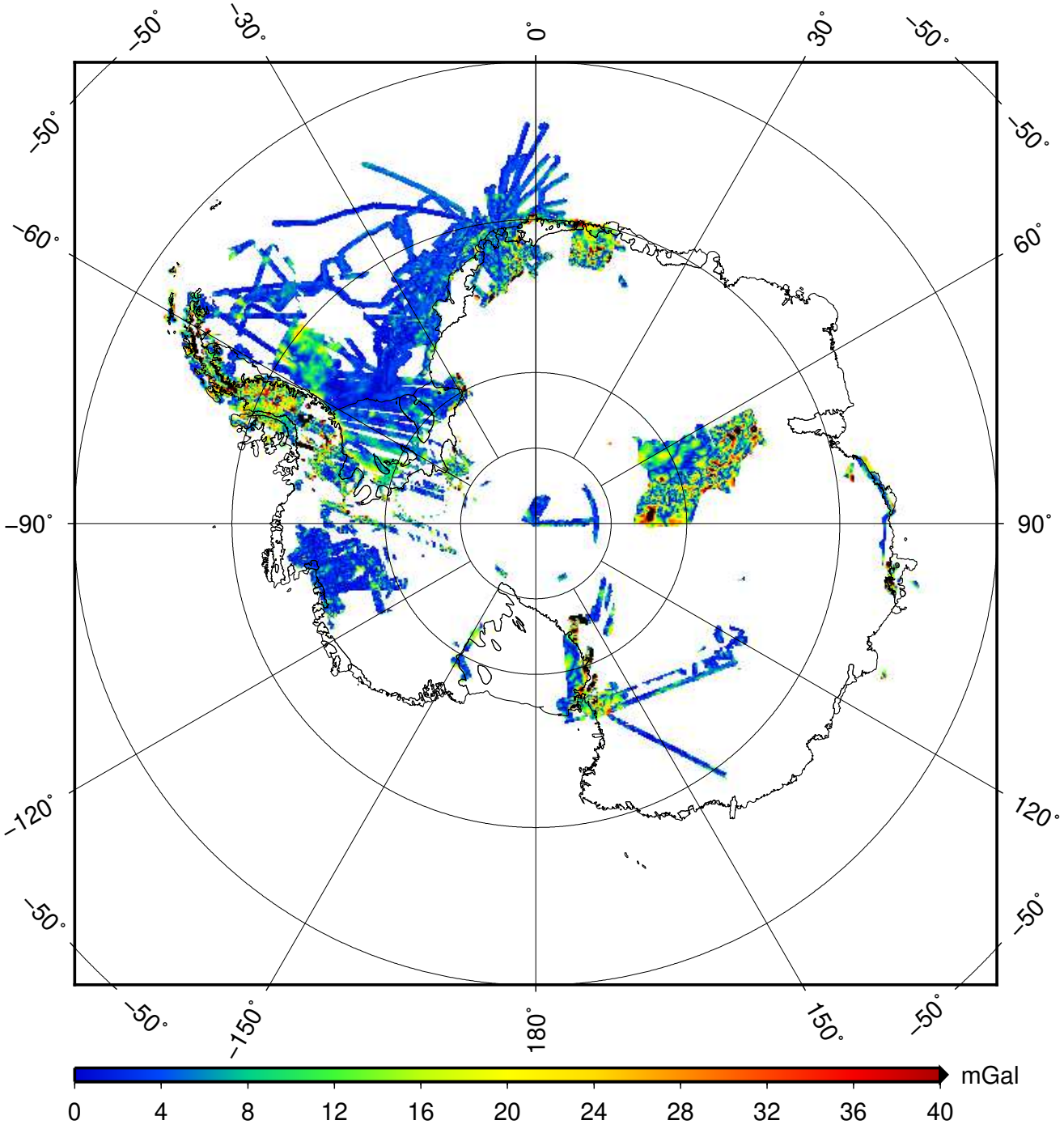

Figure S3. RMS of residual individual datasets w.r.t. residual gridded dataset. See Sect. 5 for explanations.

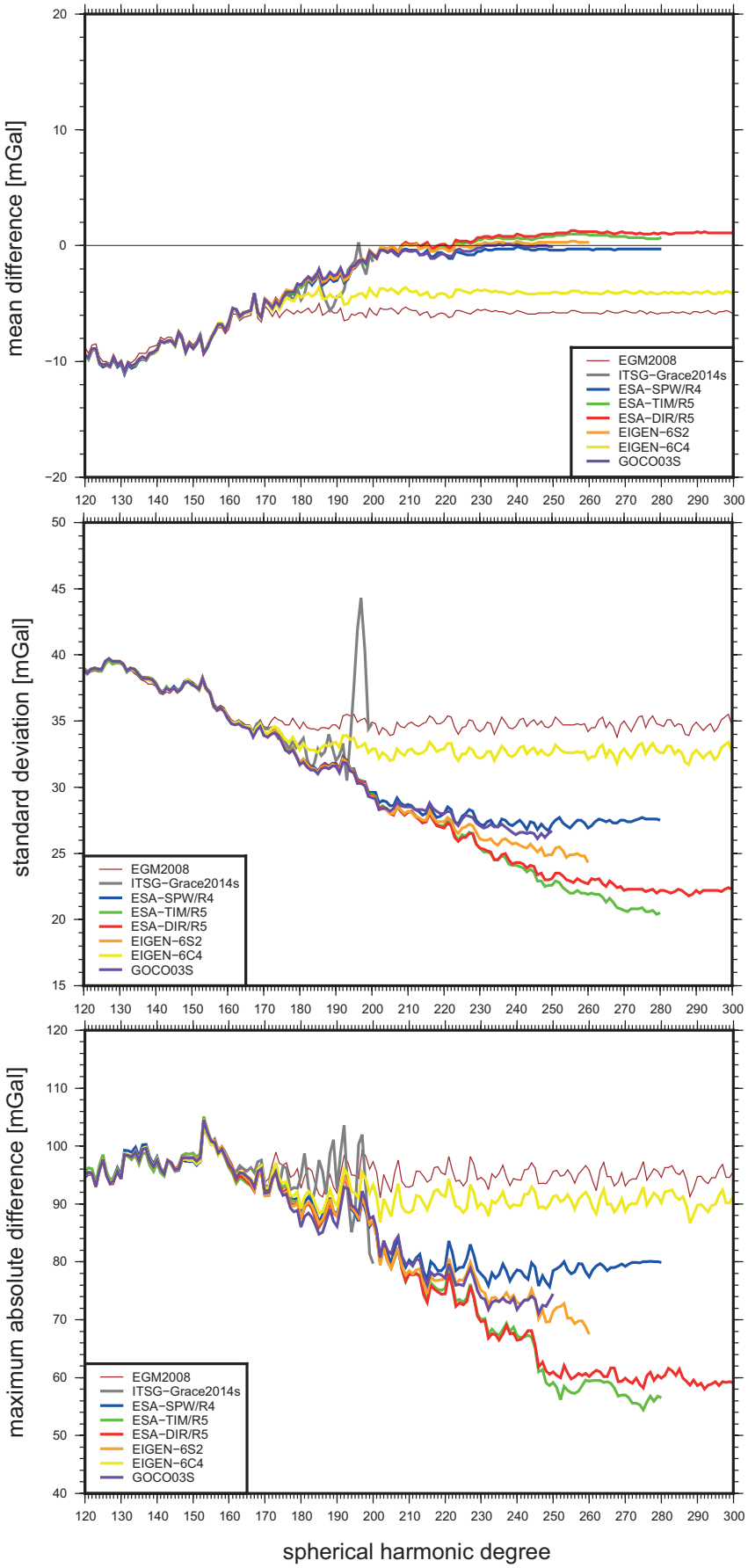

Figure S4. Mean difference (upper panel), standard deviation (middle panel) and maximum difference (lower panel) of the residual gravity disturbances (airborne data minus respective EGM harmonic series expansion truncated at certain maximum degree) for the Lake Vostok survey. Details see Subsection S2.1.

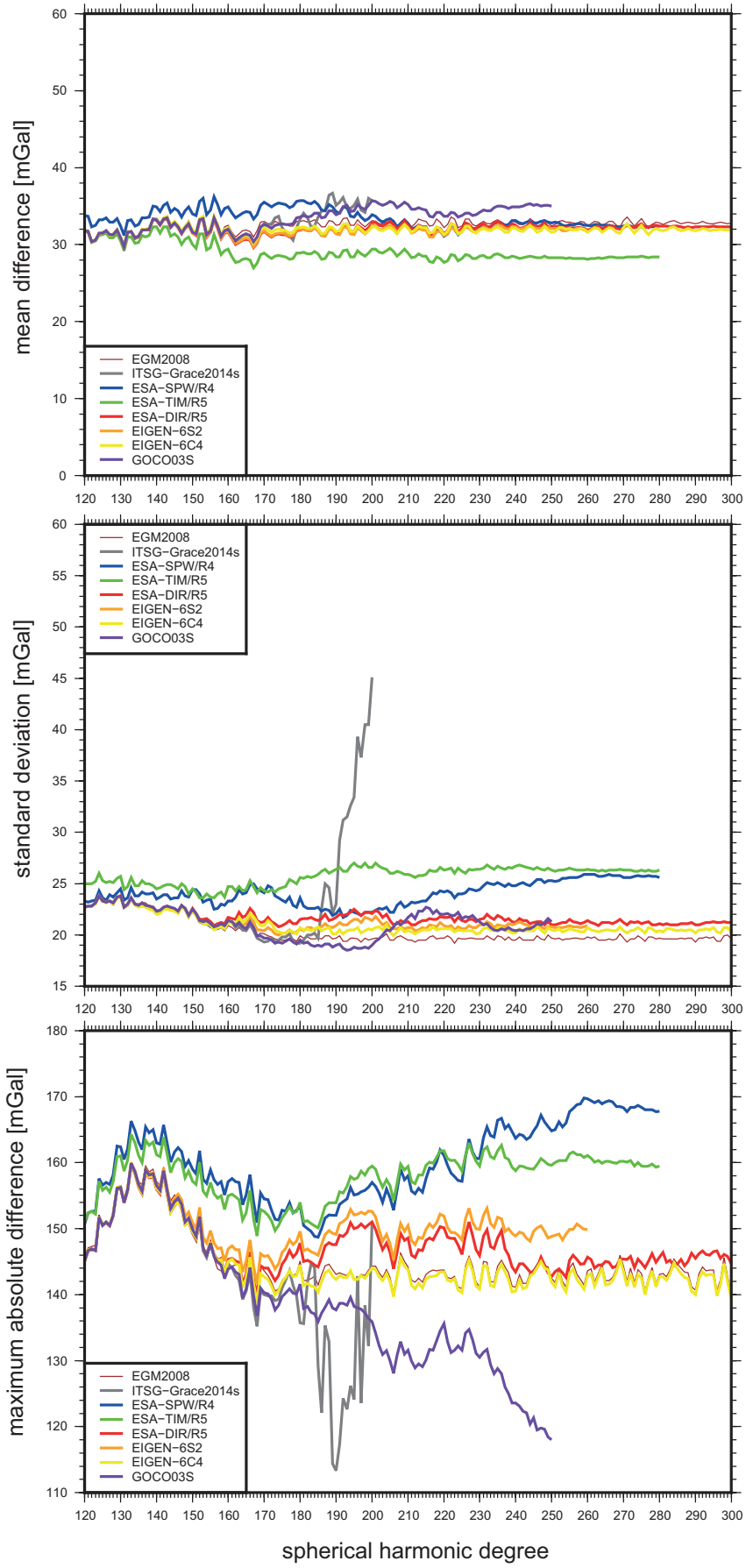

Figure S5. Mean difference (upper panel), standard deviation (middle panel) and maximum difference (lower panel) of the residual gravity disturbances (airborne data minus respective EGM harmonic series expansion truncated at certain maximum degree) for the Pensacola Pole Transect survey. Details see Subsection S2.2.